Contract No:

This document was prepared in conjunction with work accomplished under Contract No. 89303321CEM000080 with the U.S. Department of Energy (DOE) Office of Environmental Management (EM).

Disclaimer:

9. PERFORMANCE EVALUATION

This chapter summarizes the results of PA compliance against all relevant PA POs and measures. The final inventory limits presented in Chapters 7 and 8, as well as the methodology employed, provide assurance that POs will be met throughout the compliance periods. Deterministic and stochastic closure analyses also demonstrate a minimal likelihood of exceeding POs. Potential peaks post compliance are also addressed where future work is proposed to improve the understanding in actual uncertainties.

- **Section 9.1.1** summarizes predicted peak doses and concentrations versus POs for the compliance and post-compliance periods.
- **Section 9.1.2** provides details on the deterministic and stochastic closure analyses completed using a 2065 projected closure inventory for all ELLWF DUs. The deterministic results support the final inventory limits, while the stochastic results yield insight into the probability of exceeding POs.
- **Section 9.2** discusses the primary uses of the PA2022 results and interpretations.
- **Section 9.3** outlines potential future work intended to strengthen the assessment that continued operations of the ELLWF will, at a higher level of confidence, be protective of human health and the environment.

KEY TAKEAWAYS

- ✓ **Both deterministic and stochastic closure analyses are performed using final inventory limits provided in Chapters 7 and 8.**
- ✓ **Projected closure inventories for all DUs are generated based on ~26 years of ELLWF operational history.**
- ✓ **Deterministic analyses indicate that no POs will be exceeded during all compliance periods when the assumptions employed remain valid.**
- ✓ **Detailed analyses are performed to obtain biases and uncertainties associated with waste generator inventory estimates that are supplied to CWTS.**
- ✓ **When DU compositions at closure and waste generator inventory uncertainties are considered, the probability that a PO will be exceeded during its compliance period is less than 3%.**
- ✓ **For certain DUs and GW pathways, POs are exceeded during the post-compliance periods. More detailed modeling as part of future work may significantly reduce these peak doses.**

9.1. COMPARISON OF RESULTS TO PERFORMANCE OBJECTIVES

Deterministically, a tight coupling exists among CWTS inventory limits, POs, and projected closure inventories. Specifically, no PO can be exceeded during its compliance period when the assumptions employed in the deterministic analyses remain valid. However, when biases and uncertainties are included, there will exist some finite probability of exceeding one or more POs during their corresponding compliance periods. To quantify this exceedance probability event, a stochastic analysis using a Monte Carlo approach is included along with the deterministic analysis. Details and results associated with the deterministic and stochastic analyses are presented in Section 9.1.2; supporting data and material are provided in Appendix I.

The closure analysis assumes the ELLWF will be in operation and receiving waste disposals through September 2065. Within the compliance periods, both deterministic and stochastic analyses are performed. However, only deterministic analyses are discussed during the post-compliance period. The deterministic and stochastic analyses address all major exposure pathways of concern (i.e., GW, IHI, air, and radon). The POAs are pathway dependent as reported in Table 1-2. In this set of analyses, 27 operating, closed, and future DUs are considered; all DUs are assumed to be closed as of September 2065 with each DU having reached its upper activity capacity. Initially a total of 34 DUs were being considered; however, during the analyses to account for plume overlap associated with neighboring DUs, six of the DUs residing within the eastern sector of the ELLWF have been excluded from further consideration. A complete set of analyses, along with inventory limits, have been performed for the remaining 27 DUs.

The ELLWF is operated based on activity constraints imposed at the DU level. The inventory limits system employed by SWM utilizes PIFs for the GW and air pathways to implicitly address dose and concentration impacts at the POAs. Note that the POAs for the IHI and radon pathways are located within the DU and at the ground surface, respectively, and do not require application of PIFs. The methodology employed to develop the inventory limits system automatically handles dose and concentration impacts at the POAs regardless of each DU's composition up to its activity capacity limit. Chapter 8 provides the activity capacity limits for the DUs, which constrain, in a deterministic manner, total dose and concentration at the POAs so that no POs are exceeded along the POAs during the various compliance periods.

Based on a review and assessment of the deterministic results, the activity capacity of every ELLWF DU is limited by certain GWP exposure scenarios. Specifically, activity capacity is limited either by the beta-gamma or gross-alpha GWP exposure scenarios. All 27 PA2022 DUs are limited by beta-gamma except for ET02, ET03, ET05, ET07, ET08, and ET09, which are limited by gross-alpha.

The GWP exposure scenarios are significantly more limiting than the other pathways of concern. This is clearly observed for each DU when the total SOFs by pathway are compared. The average behavior, as measured by the ratio of the total SOF for a specific exposure pathway to the total SOF for the GW pathways, is given on a percentage basis as follows:

- **All-Pathways:** 6.6%
- **IHI:** 3.4%
- **Air:** 0.284%
- **Radon:** 0.0046%

As the above ratios indicate, the GWP exposure scenarios are, on average, more than one order in magnitude more limiting. Even though the GWP exposure scenarios are dominant with respect to dose and concentration impacts at their POAs, the deterministic and stochastic analyses presented below address all the exposure pathways of concern (except, as noted, for impacts during the post-compliance period when only GW pathways are considered).

Note that the level of analysis chosen depends on operational objectives. For example, in many GW cases, only Tier-3 (generic waste form) flow and transport modeling of parent radionuclides is performed initially. When additional activity capacity is desired, a GW Tier-4 (SWF) analysis is considered.

9.1.1. Impact of Final Inventory Limits

Final inventory limits for all 27 DUs are provided for the GW, IHI, air, and radon pathways in Chapters 7 and 8, and Appendices G and H. These final inventory limits impose upper-bound inventory levels within each DU at closure. The following summary of the deterministic and stochastic closure analyses is provided below:

- **Impact Within Compliance Periods:** Both deterministic and stochastic dose and concentration impacts at the compliance points are discussed for Years 0 to 1,171.
- **Impact During Post-Compliance Periods:** Only deterministic dose and concentration impacts at the compliance point are discussed for Years 1,171 to 10,171.

PORFLOW results beyond Year 10,171 are available but are not explicitly shown below.

9.1.1.1. Impact Within Compliance Periods

The compliance case represents a deterministic analysis where the following three key aspects are employed:

- 2-D and 3-D PORFLOW flow and transport analyses (Chapter 5), where a hybrid set of parameter settings are used. Certain key parameters are set to bounding values, while the remainder are set to their best-estimate values.
- Projected future DU inventories at closure are established assuming that each DU reaches its activity capacity limit.
- Waste inventories input into the CWTS database by waste generators are adjusted to account for estimated biases.

Table 9-1 summarizes the results of the 1,000-year compliance case which demonstrates that the ELLWF will meet each PO during each compliance period of concern. Also included in Table 9-1 are the results associated with a 10,000-year assessment case. Some POs are exceeded beyond the compliance periods for the LAWV and NR26E.

Peak doses and concentrations for each compliance period for all exposure pathways of interest are listed in Table 9-1. The POAs and associated compliance periods for each pathway can be found in Table 1-2. The best-estimate, projected, CWTS inventories at closure and the biases in waste-generator inventories are explicitly handled in the deterministic results reported in Table 9-1. Conversely, modeling biases are handled implicitly based on choices made in model parameter settings. Section 9.1.2.4.1 provides further discussion on the results in Table 9-1.

Table 9-1. ELLWF PA Deterministic Results for All Exposure Scenarios for Compliance and Assessment Periods

Exposure Scenario	Protection Group	Performance Objective or Measure	Performance Assessment Results					
			1,000-Year Compliance Case [a]			10,000-Year Assessment Case [b]		
			Peak Time [e] (Year)	PA Deterministic Result	Maximum DU Contributor	Peak Time [e] (Year)	PA Deterministic Result	Maximum DU Contributor
Air Pathway	Air Pathway MOP Dose	10 mrem yr^{-1} [c]	1,171	2.66x10^{-2} mrem yr^{-1} [c]	NR26E	5,302	0.131 mrem yr^{-1} [c]	NR26E
Radon Pathway	Radon Release	20 pCi m^{-2} s^{-1}	171	7.93x10^{-3} pCi m^{-2} s^{-1}	ST06	171	7.93x10^{-3} pCi m^{-2} s^{-1}	ST06
All-Pathways	All-Pathways MOP Dose	25 mrem yr^{-1}	1,171	1.35 mrem yr^{-1}	ET08	4,047	251.6 mrem yr^{-1} [f,g]	NR26E
Water Resources: • Beta-gamma • Gross-alpha [d] • Ra-226 + Ra-228 • Uranium (total)	South Carolina Groundwater Protection Standard	4 mrem yr^{-1} 15 pCi L^{-1} 5 pCi L^{-1} 30 µg L^{-1}	43 1,171 1,171 1,171	2.59 mrem yr^{-1} 6.61 pCi L^{-1} 1.68x10^{-3} pCi L^{-1} 2.95x10^{-9} µg L^{-1}	ST24 ET08 ET08 ET08	4,198 3,496 7,940 10,171	16,106 mrem yr^{-1} [f,g] 30.5 pCi L^{-1} [f] 2.18 pCi L^{-1} 1.26x10^{-5} µg L^{-1}	NR26E LAWV ILV ST24
Inadvertent Human Intruder: • Chronic exposure • Acute exposure	Chronic IHI Dose Acute IHI Dose	100 mrem yr^{-1} 500 mrem	171 171	68.3 mrem yr^{-1} 0.751 mrem	NR26E ST23	171 171	68.3 mrem yr^{-1} 0.751 mrem	NR26E ST23

Notes:

[a] The prescribed end time for compliance assessment is 1,000 years beyond the end of IC (Year 171) [i.e., Year 0 to Year 1,171 overall compliance period].

[b] The prescribed end time for informational assessment is 10,000 years beyond the end of IC (Year 171) [i.e., Year 0 to 10,171 overall assessment period).

[c] Excluding radon in air.

[d] Including Ra-226 but excluding radon and uranium.

[e] Peak time relative to the start of ELLWF operations on September 28, 1994.

[f] Peak value exceeds PO. Exceedance occurs beyond the compliance periods but within a 10,000-year period after the end of IC.

[g] Computed doses dominated by neutron-activated Ni-59S disposed in Naval Reactor components. Dose impacts can be reduced by refinement of pessimistically leaning model employed.

A stochastic closure analysis has also been performed, explicitly incorporating (1) uncertainties associated with the projected closure inventories (i.e., a DU's final composition) and (2) waste-generator inventories (i.e., inventory determinations). Model uncertainties are handled implicitly based on the choices made in model parameter settings. All four primary exposure pathways (GW, IHI, air, and radon) are included in the stochastic analysis.

Figure 9-1 displays the exceedance probability curve for 10,000 MC simulations. Key elements of the exceedance probability curve include:

- The maximum total SOF is ~0.69 at an exceedance probability of 50% (31% margin from the POs while remaining within the compliance periods.
- The exceedance probability is ~2.9% for a maximum total SOF of 1.0 (reasonably low likelihood of exceeding any POs during the compliance periods).
- A protracted tail beyond 2.9% is consistent with the log-normal distributions assumed to address projected inventory uncertainties.

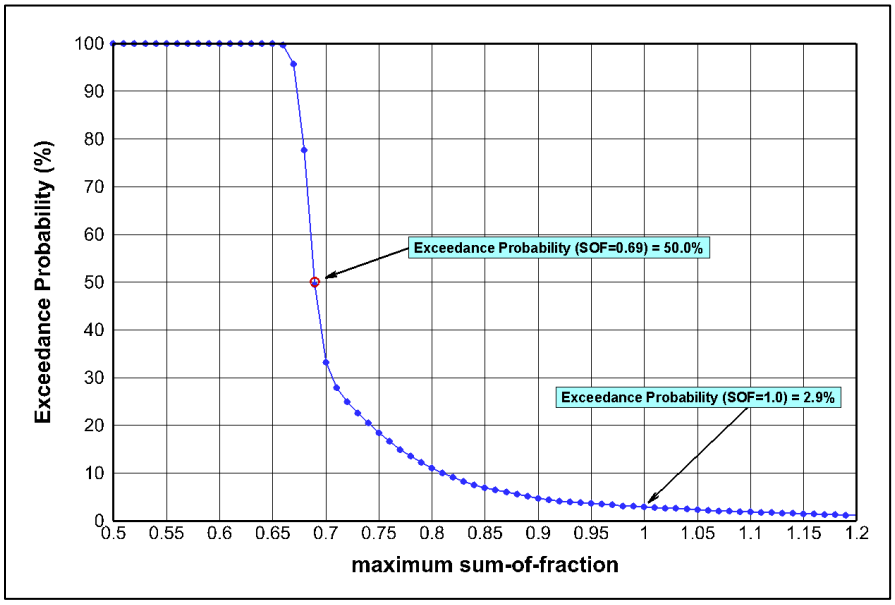

Figure 9-1. Closure Exceedance Probability Beyond a Specified Maximum Sum-of-Fractions for E-Area Low-Level Waste Facility

MC methods are quite versatile but are typically slow to converge when simulating low-probability events. For this PA, multiple trial sets of MC simulations comprising an increasing number of realizations were executed to assess the minimum number of realizations required. The results of the screening trial (not reported) deemed 10,000 MC realizations to be adequate. However, to further evaluate whether a MC simulation comprised of 10,000 realizations is adequate for determining the probability of exceeding a total SOF of 1.0, the cumulative exceedance probability was computed for each subsequent MC realization, along with a running average. The results of this computation are displayed in Figure 9-2. For this low-probability event, the exceedance probability varies greatly during the first ~2,000 MC realizations (green circles). Beyond the initial

2,000 realizations, a running average is computed for the subsequent MC realizations (red curve). The results in Figure 9-2, as well as the prior trial runs based on 10,000 MC realizations, indicate that the probability of exceeding a SOF of 1.0 is approximately 3% or less.

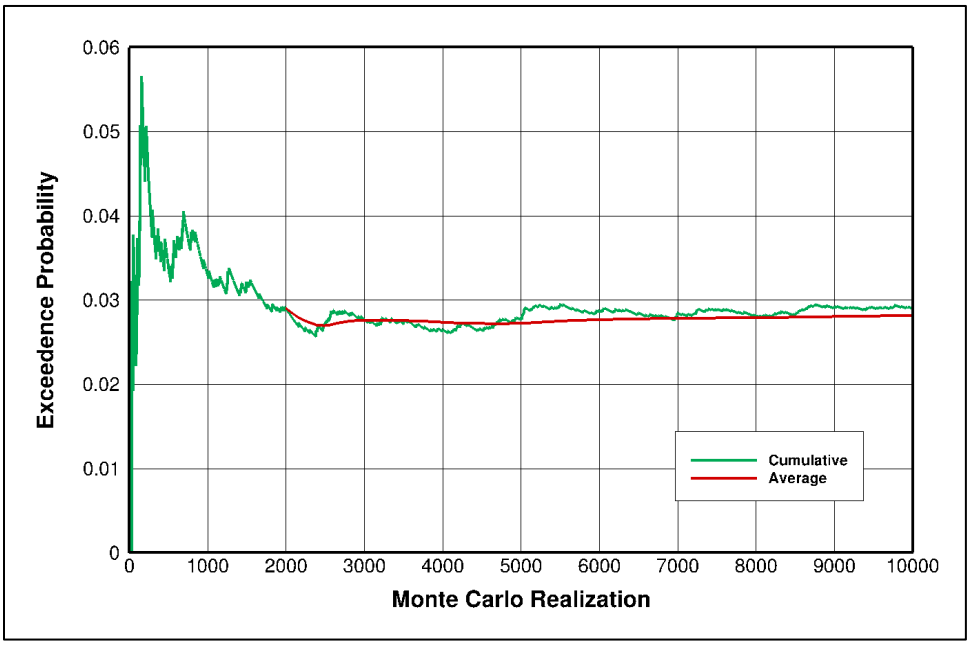

Figure 9-2. Probability of Exceeding a Sum-of-Fractions of 1.0 during Monte Carlo Simulation

Details associated with the summary results presented in Table 9-1 and Figure 9-1 are provided in Section 9.1.2. Supporting information is also provided in Appendix I.

9.1.1.2. Impact During Post-Compliance Periods

U.S. DOE (2021b) specifies that a PA should evaluate compliance with POs for a 1,000-year period after facility closure. Under current SRS site plans, operational closure of the ELLWF is estimated to be September 2065. Additionally, U.S. DOE guidance in DOE-STD-5002-2017 (U.S. DOE, 2017) recommends that potential peaks during the post-compliance period be addressed. U.S. DOE (1999) states the following:

"Although the period of performance (i.e., the time over which the performance assessment is to provide reasonable expectation of compliance with the performance objectives) is 1,000 years, it may be helpful to extend the calculation to include the maximum impact (i.e., peak dose), even if the maximum is not realized for tens of thousands of years. This calculation may increase the understanding of the models used and the disposal facility performance but are not used for determining compliance with the disposal performance objectives."

To address performance aspects during the post-compliance period, all GW transport calculations are performed until the time when peak radionuclide concentrations occur or, in the case of STs and ETs, for up to ~10,000 years beyond the end of IC. Simulation times vary because half-lives and absorption characteristics differ significantly among the parent radionuclides and their

progeny. In general, PORFLOW transport analyses use the following simulation durations beyond the end of IC in 2165:

- **Engineered Trenches:** 10,300 years for most DUs and radionuclides (4,129 years for more mobile and shorter half-life cases).
- **Slit Trenches:** 10,000 years for all DUs and radionuclides.
- **LAWV and ILV:** 50,000 years for all DUs and radionuclides.
- **NRCDAs** – 10,000, 30,000, 100,000, and 150,000 years for various DUs and radionuclides.

Section 9.1.2.4.2 discusses deterministic results spanning 10,000 years beyond the end of IC. For many DUs and exposure pathways, the POs are still met across the entire post-compliance periods. This is true for any ELLWF DU in the case of the IHI, air, and radon pathways. However, for the GW pathways, the following exceedances are observed as rank ordered by peak SOF (peak values of SOF listed in parentheses):

- **Beta-Gamma:** NR26E (4,027); NR07E (267); ILV (10); ST14 (6); LAWV (2)
- **Gross-Alpha:** LAWV (2.0); ILV (1.2)
- **All-Pathways:** NR26E (10.1); ILV (1.5)

Section 9.1.2.4.2 provides the dose/concentration history time profiles for each of the above exceedances.

9.1.2. Closure Analysis

This section outlines the details associated with the ELLWF closure analysis; supporting information is included in Appendix I.

9.1.2.1. Computational Strategy

Deterministic and stochastic closure analyses are employed in this PA to demonstrate overall ELLWF compliance with POs. The deterministic analyses impose inventory constraints that are consistent with the CWTS limits system (i.e., final inventory limits by exposure pathway provided in Chapters 7 and 8). A stochastic approach to address ELLWF compliance has been utilized in the past. For example, a UDQE by Hamm et al. (2013) addressed the potential use of existing ST12 inventory limits to bound the new ET03; stochastic calculations were performed using a Microsoft Excel[1] model. In addition, Hamm et al. (2018) completed an SA in 2018 that addressed concerns associated with the new calibration of the aquifer flow field beneath the eastern sector of the ELLWF. Due to the added complexities, the Microsoft Excel model was converted to a FORTRAN algorithm.

The closure analysis in this PA updates and extends the FORTRAN algorithm implemented by Hamm et al. (2018) and explicitly addresses all four exposure pathways (GW, IHI, air, and radon)

[1] Microsoft, Excel, and Word are trademarks of the Microsoft group of companies.

as defined in Table 1-2 for the 27 ELLWF DUs. Section I.3 in Appendix I describes the Closure Analysis Toolkit in detail.

Given the inherent uncertainties associated with inventories and their projection to calendar year 2065, the supplemental stochastic approach to closure analysis is deemed warranted. The basic closure analysis strategy employs the following the steps:

Initial Setup

1. Existing CWTS radionuclide inventories for operating and closed DUs are input.
2. DU-specific radionuclide inventory limits for every pathway are input for each CWTS time window (taken from Chapters 7 and 8).
3. Dose-factor history time profiles are input for the GW pathways and are computed from transient aquifer concentrations that vary spatially over the entire 100-meter POA. The output of these concentrations is recorded in PORFLOW HIST files.
4. Transient dose factors are input for the IHI pathways and are computed from soil concentrations within the waste zone of a DU.
5. Transient dose factors are input for the air pathway and are computed for plume concentrations at the 100-meter POA from volatile radionuclides emanating from a DU.
6. Transient dose factors are input for the radon pathway and are computed from the flux of Rn-226 at the surface of each DU. All parent radionuclides that produce Rn-226 are included.
7. Biases and uncertainties associated with waste-generator inventories are input for every parent radionuclide on a DU basis.
8. Log-normal distributions or composition vectors associated with the 2065 projected closure compositions within each DU are input.

Deterministic Simulation

1. DU-specific, best-estimate composition vectors (CWTS closure inventories) are imposed. The composition vector is comprised of an existing inventory vector (operating or closed DU) and a projected inventory vector (operating or future DU). The existing inventory vector is based on CWTS inventories supplied by the waste generators.
2. DU-projected inventory vectors are adjusted such that a total maximum SOF of 1.0 is achieved for a limiting pathway within a CWTS time window. For the GW and air pathways, inventory limits include PIFs.
3. The resulting, projected CWTS closure inventories are adjusted using bias multipliers (≤ 1).
4. The maximum dose and peak time for each GW, IHI, air, and radon pathway are computed using the CWTS-adjusted closure inventories.
5. Plots of ELLWF GW pathway doses along the North curtain are generated at the peak time. Plots of transient GW pathway doses for the top-ten DUs sorted by peak doses are generated at the element on the curtain where the DU peak dose occurs.

6. Plots of transient acute and chronic IHI pathway doses are generated for the top-ten DUs with peak doses.
7. Plot of transient air pathway doses is generated for the top-ten DUs with peak doses and the total for the ELLWF.
8. Plot of transient radon pathway doses is generated for the top-ten DUs with peak doses.
9. Plots of transient DU pathway doses are generated for the top-ten contributing radionuclides. The transient DU total doses are also plotted. Transient doses at the element of peak dose on the North curtain are plotted for GW pathways.

Stochastic Simulations (Monte Carlo Method)

1. DU-specific closure composition vectors are generated for each MC realization. The composition vector is comprised of an existing inventory vector (open or closed DU) and a projected, stochastic inventory vector (open or future DU). The existing inventory vector is based on CWTS inventories supplied by the waste generators. The projected stochastic inventory vector is randomly sampled from a log-normal distribution (ST and ET) or determined from a composition vector computed from an existing inventory (LAWV, ILV, and NR26E). The projected stochastic inventory vector is normalized to a unit composition (Ci per Ci).
2. CWTS inventory uncertainties are randomly sampled from a gaussian distribution for each radionuclide within the DU.
3. For a closed DU, CWTS inventory biases and uncertainties are applied to existing inventories to produce the stochastic closure inventories.
4. For an open or future DU, a future SOF vector (w) is computed for each pathway within a CWTS time window using the unit composition vector (n) and the reciprocal of each member of the inventory limits matrix (w by n), where n is the number of radionuclides in the DU and w is the number of CWTS time windows. The future SOF vector is scaled and added to an existing SOF vector until a total SOF of 1.0 is achieved for the limiting pathway within a CWTS time window. The CWTS projected total inventory is the sum of the scaled unit composition and the existing inventory. The stochastic closure inventory is the product of the CWTS inventory bias and uncertainty applied to the CWTS projected total inventory.
5. The maximum total SOFs for each GW, IHI, air, and radon pathway are computed using stochastic closure inventories at each MC realization. A maximum total SOF of all pathways is further computed. The maximum total SOFs for each realization and pathway are stored at the ELLWF and DU level in csv files. The csv files are postprocessed to create histograms of maximum SOF for significant pathways. The files are further processed to create mean, standard deviation, and the coefficient of variation for each pathway within a DU and the ELLWF. The maximum total SOF over all MC realizations is located at realization number (r_{max}), which is used to retrieve stochastic closure inventories for dose output processing.
6. Plots of maximum SOF as a function of MC realization are generated for each pathway at the ELLWF and DU level.

7. Plots of total SOF as a function of MC realization are generated for each pathway within a CWTS time window at the DU level.
8. Plots of ELLWF GW pathway doses along the North curtain are generated at the peak time for realization r_{max}. Plots of transient GW pathway doses for the top-ten DUs sorted by peak doses are generated at the element on the curtain where the DU peak dose occurs.
9. Plots of transient acute and chronic IHI pathway doses are generated for the top-ten DUs with peak doses for realization r_{max}.
10. Plot of transient air pathway doses is generated for the top-ten DUs with peak doses and the total for the ELLWF for realization r_{max}.
11. Plot of transient radon pathway doses is generated for the top-ten DUs with peak doses for realization r_{max}.
12. Plots of transient DU pathway doses are generated for the top-ten contributing radionuclides for realization r_{max}. The transient DU total doses are also plotted. Transient doses at the element of peak dose on the North curtain are plotted for GW pathways.

This stochastic closure analysis directly addresses the following two uncertainties:

- Uncertainties associated with the projected September 30, 2065, closure inventories but constrained to conform to the CWTS inventory limits.
- Parent radionuclide uncertainties and biases associated with the values supplied by waste generators.

Note that model biases and uncertainties are not explicitly addressed in the deterministic or stochastic closure analysis simulations. Instead, the DU-specific inventory limits are employed as deterministic values where overall conservatism exists because of the following conditions and assumptions:

- All inventory burials for a specific DU are assumed to occur at the time of first burial, where (1) actual decay of parent radionuclides and (2) the spreading of burials over a DU operation would actually reduce doses at the POAs. The actual time delay of waste assessment by waste generators and subsequent actual burial in the ELLWF can be months to years, yet no activity reductions are applied to CWTS inventories.
- Bounding surface infiltration rates are employed where the closure cap degradation rate is much higher than expected.
- The PIF approach provides SWM flexibility in the timing associated with opening and closing specific DUs and employs steady-state transport analyses to obtain upper-bound estimates of plume overlap. The actual transient nature can significantly reduce doses at the 100-meter POA for the various GW pathways.
- For parent radionuclides with progeny, the maximum concentrations at or beyond locations along the 100-meter POA are not required to coincide. This yields maximum doses at the 100-meter POA that exceed their values if dose was instead computed only at the location of maximum parent concentration.

- The PA methodology employed establishes GW inventory limits using PORFLOW VZ and aquifer models in which some parameter settings for the nominal PA case simulations are not at their best-estimate values but are instead skewed in a pessimistically leaning direction (typically referred to as a "hybrid" approach).
- Subsidence of all non-crushable containers residing in a given ST and ET is assumed to occur simultaneously immediately after final closure cap installation at the end of IC.
- Closure analyses assume that every DU is filled to its activity capacity at ELLWF operational closure. Historical data suggest that essentially all DUs reach their volume capacity first (see Chapter 8 where the historical, average, activity-to-volume capacity ratios are 90% for STs and ETs, 28% for the LAWV and ILV, and 13% for NRCDAs).
- For the GW pathways, there are a small, limited number of nonoverlapping time windows employed in generating GW inventory limits: NR07E (one beta-gamma, one gross-alpha, one radium, one uranium, and one all-pathways); LAWV, ILV, and NR26E (two beta-gamma, one gross-alpha, one radium, one uranium, and two all-pathways); STs and ETs (three beta-gamma, one gross-alpha, one radium, one uranium, and two all-pathways). Thus, an embedded degree of margin exists between the actual peak doses at the 100-meter POA and those imposed via the time-window approach.
- Minimum soil thicknesses in IHI pathways calculations are used to represent soil covers.
- Maximum transient concentrations from first and last burial timing are generated for IHI pathways calculations.
- Waste removal from waste zones by mechanisms associated with other exposure pathways are neglected. For example, the IHI, air, and radon pathways analyses assume zero leaching of waste into infiltrating GW.
- In many cases, the IHI pathways analyses do not include the additional gamma-ray shielding associated with engineered barriers such as concrete and metal containers.
- The radon pathway analyses assume no lateral spreading of constituents; only vertical migration in a 1-D model is employed.
- For air pathway analyses, the DU source terms are assumed to be point sources and atmospheric plume overlap is assumed to be aligned to a single point receptor located 100 meters downwind.

Plume overlap is directly accounted for in calculating the maximum total SOF at the 100-meter POA for the GW pathways because concentration profiles along the 2-D curtains are employed for each DU (i.e., PORFLOW HIST files are generated along the 100-meter POA where the aquifer concentrations for each parent and its progeny are stored at every time step). For each parent radionuclide, the summed DU contributions along the 2-D curtains address plume overlap directly.

Because final inventory limits for the air pathway are not limiting, a quite conservative (pessimistically leaning) assumption is made for atmospheric plume overlap. All 27 PA2022 DUs are assumed to be located 100 meters upstream of the POA and their maximum concentrations have a single, common point on that 100-meter POA.

The following exposure pathways (and time windows, where appropriate) are explicitly addressed in the deterministic and stochastic analyses:

- GWP (beta-gamma, gross-alpha, radium, and uranium)
- All-pathways
- IHI (acute and chronic)
- Air
- Radon

The time periods considered are as follows:

- **Deterministic Analyses:** Year 0 to Year 1,171 (across the entire set of compliance periods) and varying time periods post compliance while chasing the peak doses and concentrations.
- **Stochastic Analyses:** Year 0 to Year 1,171 (across entire set of compliance periods).

9.1.2.2. Uncertainty in Disposal-Unit Compositional Vector

A final inventory of parent radionuclides is predicted for every currently open and future DU at the time of operational closure in 2065. To estimate projected closure inventories, the assumption is made for each currently open DU that generic waste disposed in that DU in the future will have the same gross radionuclide composition as the waste placed in that specific DU as of March 31, 2021 (current CWTS inventory). This means that the generic waste form composition fractions of individual, currently open DUs will be the same at operational closure as they were on March 31, 2021. For future DUs, for which no current inventory exists, generic waste form composition fractions are estimated by averaging the parent radionuclide compositions of all closed DUs of similar type, together with the projected final compositions of all open DUs of similar type.

In the absence of specific information on variability in the parent radionuclide compositions of generic waste form packages, the uncertainty in the predicted compositional vectors is characterized using the variability between compositional vectors of both closed and open DUs of similar type. This approach worked for STs and ETs because waste composition data exist for six closed and eight open STs and ETs. Broadly speaking, the same kinds of generic waste have been placed in these 14 ST and ET DUs and will continue to be placed in the remaining ST and ET DUs. Unfortunately, the same cannot be said for the LAWV, ILV, and NR26E. Each of these DUs has unique wastes, so comparison with the compositions of other DUs does not provide a meaningful basis for estimating uncertainty.

Table 9-2 displays average, generic waste form, radionuclide inventories as well as their standard deviations at closure calculated for the 14 STs and ETs that currently contain disposed waste. Columns 2 and 3 consider the waste inventories in the 10 STs only; columns 4 and 5 consider waste inventories in the four ETs only; and columns 6 and 7 display the same statistics for all 14 STs and ETs combined. The ratio of the standard deviation to the average inventory is also calculated for the 14-trench case (last column).

The last two rows in Table 9-2 present data for two SWFs that appear in multiple existing STs and ETs and for which future disposals are anticipated (U-233D and C-14N). These are highlighted in green because their disposal limits are different than those for generic waste. Depleted uranium waste (U-233D) is disposed in both STs and ETs, while used NR coolant pumps (C-14N) are limited to STs. Because multiple emplacements already exist, there are sufficient data for a statistical analysis.

The last column in Table 9-2 represents the variability in each parent radionuclide per Ci buried. This ratio of standard deviation to the arithmetic mean is used to scale the standard deviation of each parent radionuclide of a specific ST or ET back to the average standard deviation value as follows:

$$S_{ij} = I_{ij}\left(\frac{\overline{S}_i}{\overline{I}_i}\right) \qquad \text{Eq. (9-1)}$$

where:

S_{ij} Scaled standard deviation of inventory for i^{th} parent radionuclide in j^{th} ST and ET (Ci)

I_{ij} Inventory of i^{th} parent radionuclide in j^{th} ST and ET (Ci)

$\overline{S}_i$ Standard deviation of i^{th} parent radionuclide from 7th column in Table 9-2 (Ci)

$\overline{I}_i$ Average inventory of i^{th} parent radionuclide from 6th column in Table 9-2 (Ci)

Note that the quotient in parentheses in Eq. (9-1) is tabulated in the last column in Table 9-2. (For the LAWV, ILV, and NR26E, the scaled standard deviation for each parent radionuclide is set equal to zero because no relevant variability information is available.)

In the majority of cases for the 14 STs and ETs in Table 9-2, calculated standard deviations for inventories of generic-waste-form radionuclides at closure are greater than their corresponding arithmetic means (as indicated by $\left(\overline{S}_i/\overline{I}_i\right) > 1$). This means that MC simulations based on individual parent radionuclide inventories generated from these means and standard deviations will often result in physically meaningless negative values if a normal distribution is assumed. To avoid this situation, the scaled standard deviations from Eq. (9-1) are used together with the parent radionuclide inventories within each ST and ET to compute log-normal distributions instead.

Table 9-2. Average and Standard Deviations of Generic Waste Form Radionuclide Inventories in Slit and Engineered Trenches

Radionuclide	Closed and Open STs Only		Closed and Open ETs Only		Closed and Open STs & ETs Combined		
	Average	Std Dev	Average	Std Dev	Average	Std Dev	Std Dev/Average
	(Ci)						(-)
Ag-108m	3.74E-05	1.12E-04	6.36E-06	8.86E-06	3.03E-05	9.95E-05	3.28627
Am-241	9.89E-01	1.22E+00	1.30E+00	5.67E-01	1.06E+00	1.11E+00	1.04752
Am-242m	3.38E-01	7.24E-01	1.60E-01	1.11E-01	2.97E-01	6.42E-01	2.16177
Am-243	1.14E-01	2.97E-01	1.64E-02	1.46E-02	9.11E-02	2.64E-01	2.89818
Be-10	1.18E-07	3.54E-07	2.72E-10	3.85E-10	9.08E-08	3.14E-07	3.45999
C-14	3.68E-02	1.61E-02	8.34E-02	3.48E-02	4.76E-02	2.94E-02	0.61736
Cf-249	7.87E-02	1.72E-01	1.82E-02	2.57E-02	6.47E-02	1.53E-01	2.36990
Cf-251	7.16E-02	1.56E-01	1.66E-02	2.34E-02	5.89E-02	1.39E-01	2.36677
Cl-36	1.73E-06	3.09E-06	2.35E-05	3.29E-05	6.76E-06	1.85E-05	2.73109
Cm-245	1.28E-03	2.45E-03	4.96E-04	5.00E-04	1.10E-03	2.19E-03	1.98693
Cm-247	1.74E-03	3.15E-03	1.81E-04	2.52E-04	1.38E-03	2.85E-03	2.05727
Cm-248	3.30E-04	8.03E-04	1.94E-07	2.04E-07	2.54E-04	7.18E-04	2.82699
Cs-135	5.26E-08	1.17E-07	4.98E-11	6.03E-11	4.05E-08	1.05E-07	2.58582
Cs-137	5.84E+01	5.02E+01	1.18E+02	7.37E+01	7.20E+01	6.17E+01	0.85665
H-3	1.50E+00	2.37E+00	1.28E+00	6.81E-01	1.45E+00	2.11E+00	1.45344
I-129	9.93E-05	1.41E-04	1.02E-04	3.39E-05	1.00E-04	1.25E-04	1.24723
K-40	4.44E-04	1.23E-03	1.44E-04	7.63E-05	3.75E-04	1.09E-03	2.89400
Nb-94	8.24E-04	6.32E-04	1.99E-03	9.09E-04	1.09E-03	8.59E-04	0.78639
Ni-59	6.19E-02	6.68E-02	8.22E-02	2.68E-02	6.66E-02	6.06E-02	0.90945
Ni-63	1.66E+00	1.79E+00	4.37E+00	2.53E+00	2.29E+00	2.29E+00	1.00099
Np-237	8.47E-03	7.74E-03	2.52E-02	1.36E-02	1.23E-02	1.18E-02	0.95433
Pa-231	7.05E-07	2.11E-06	4.04E-06	3.84E-06	1.47E-06	2.97E-06	2.01324
Pd-107	2.37E-08	4.34E-08	5.49E-14	7.76E-14	1.83E-08	3.94E-08	2.15793
Pu-239	2.15E+00	2.02E+00	4.42E+00	2.84E+00	2.68E+00	2.43E+00	0.90872
Pu-240	5.59E-01	5.28E-01	1.15E+00	6.06E-01	6.94E-01	6.00E-01	0.86483
Pu-241	1.21E+01	1.09E+01	1.76E+01	8.72E+00	1.34E+01	1.07E+01	0.80137
Ra-226	4.12E-04	9.33E-04	1.43E-03	1.83E-03	6.46E-04	1.28E-03	1.97416
Rb-87	9.70E-12	2.50E-11	1.01E-05	1.42E-05	2.32E-06	8.05E-06	3.46409
Sn-126	7.96E-04	2.12E-03	1.58E-04	1.80E-04	6.48E-04	1.88E-03	2.89807
Sr-90	3.54E+01	5.03E+01	7.39E+01	4.69E+01	4.43E+01	5.21E+01	1.17714
Tc-99	3.80E-02	3.67E-02	6.63E-02	2.24E-02	4.45E-02	3.60E-02	0.80892
Th-229	1.05E-03	2.41E-03	9.14E-03	9.37E-03	2.92E-03	6.03E-03	2.06773
Th-230	3.04E-04	4.40E-04	4.02E-03	2.52E-03	1.16E-03	2.01E-03	1.73410
Th-231	3.77E-02	5.09E-02	4.49E-03	2.49E-03	3.00E-02	4.68E-02	1.55706
U-232	9.45E-03	1.60E-02	4.28E-02	4.24E-02	1.71E-02	2.84E-02	1.65857
U-233	6.53E-01	9.81E-01	3.62E+00	3.04E+00	1.34E+00	2.11E+00	1.57382
U-234	1.12E+00	1.25E+00	8.31E-01	4.07E-01	1.05E+00	1.12E+00	1.06624
U-236	1.75E-02	1.91E-02	1.63E-02	1.15E-02	1.72E-02	1.76E-02	1.02358
U-233D	3.56E-03	7.56E-03	1.64E-03	2.32E-03	3.12E-03	6.77E-03	2.17018
C-14N	2.12E-02	2.42E-02	--	--	--	--	1.14281

Notes:

SWF radionuclides are highlighted in green.

The relationship between the normal and log-normal mean and standard deviations is expressed as follows:

$$\mu_{ij} = ln\left(\overline{S}_i^2\right) - \frac{1}{2}\sigma_{ij}^2 \qquad \text{Eq. (9-2)}$$

$$\sigma_{ij} = \sqrt{ln\left(1 + \left(\frac{S_{ij}}{I_{ij}}\right)^2\right)} \qquad \text{Eq. (9-3)}$$

where:

μ_{ij} Log-normal distribution location parameter for i^{th} parent radionuclide in j^{th} trench (-)

σ_{ij} Log-normal distribution scale parameter for i^{th} parent radionuclide in j^{th} trench (-)

S_{ij} Scaled standard deviation value for i^{th} parent radionuclide in j^{th} trench (Ci)

I_{ij} Inventory of i^{th} parent radionuclide in j^{th} trench (Ci)

The relationships in Eq. (9-2) and Eq. (9-3) are used to generate log-normal distributions for parent radionuclides in all currently open and future STs and ETs. Example log-normal PDFs for Am-241 in seven different STs and ETs are plotted in the left image of Figure 9-3, while the corresponding CDFs are plotted in the right image of Figure 9-3. Because the scaled standard deviations for the LAWV, ILV, and NR26E are set to zero, both the normal and log-normal distributions are identical, allowing values at the projected inventory only as shown in Figure 9-4. For these three DUs, the PDFs reduce to Dirac delta functions and the CDFs reduce to Heaviside step functions at the projected inventory values.

Log-normal distribution parameters for all future parent radionuclide inventories in all DUs that can be used for MC simulation modeling are detailed in Appendix I, Section I.1.

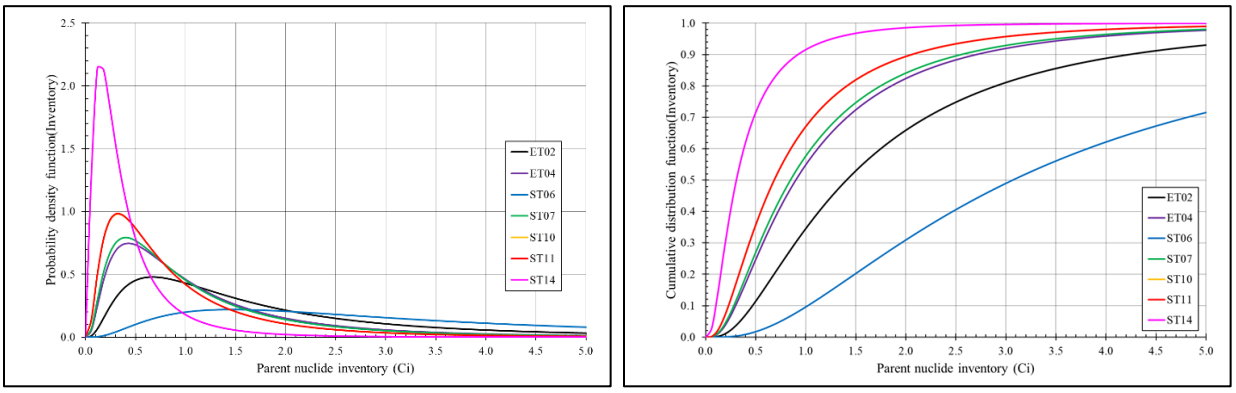

Figure 9-3. Log-Normal Probability and Cumulative Distribution Functions of Future Waste Disposals for Am-241 in Seven Slit and Engineered Trenches

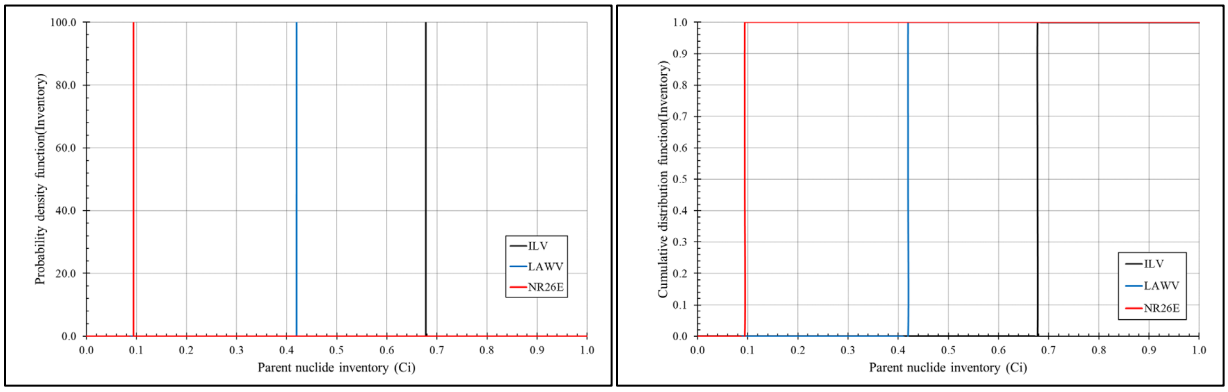

Figure 9-4. Log-Normal Probability and Cumulative Distribution Functions of Future Waste Disposals for Am-241 in ILV, LAWV, and NR26E

9.1.2.3. Bias and Uncertainty in CWTS Inventory per Radionuclide

As discussed in Section 2.3.5, the inventory values from waste generators input in CWTS have potential biases and uncertainties associated with them. These biases and uncertainties are addressed within the closure analysis by employing an additional stochastic step in the overall computational strategy as highlighted in Section 9.1.2.1.

The isotopic activity of each measured item is either measured directly for each radionuclide or it is calculated from the product of the total activity of an item and the expected isotopic distribution, which is described in the waste stream technical baseline documentation. By examining this documentation and measurement method, isotopic uncertainty and bias can be estimated. The major assumption made in this analysis is that the uncertainties are random and independent. This allows the normal distribution to be used to describe the average and uncertainty within a DU. Section 2.3.5 and Appendix B describe this process and provide an example calculation. (Taylor and Whiteside, 2022) describe the analysis in detail, show how the calculations are used and how the various assumptions are applied, and include a listing of the analysis so this method can be reproduced.

In summary, the activity (A, Ci) of a measured item using the DTC (Dose-to-Curie), RAD (Radiation weight or volume), and STC (Smear-to-Curie) methods is expressed as:

$$A = M \times C \qquad \text{Eq. (9-4)}$$

where:

M Measured activity of a waste cut or container (Ci)
C Fraction of activity associated with that radionuclide in that waste stream (unitless)

In the CBP (Characterization-by-Package) method, the quantity C equals 1.0 with no uncertainty.

Both M and C have some uncertainty in them and may be systematically biased. Therefore, the true activity (A_{true}) of a measured item can be expressed as:

$$A_{true} \pm U_{A_{true}} = A_W \times \delta_{B_A} \pm U_W = \left(M_W \times \delta_{B_M} \pm U_M\right) \times \left(C_W \times \delta_{B_C} \pm U_C\right) \quad \text{Eq. (9-5)}$$

and

$$U_W = \sqrt{U_M{}^2 + U_C{}^2} \quad \text{Eq. (9-6)}$$

where:

$U_{A_{true}}$ Relative uncertainty in the true activity of the item (Ci), equal to U_W
A_W CWTS reported activity of the item (Ci)
δ_{B_A} Product of the measurement and characterization biases (unitless)
U_W Relative uncertainty of the activity of the item (Ci), calculated by:
M_W Measurement value of the item (Ci)
C_W Characterization value of the item (unitless)
δ_{B_M} Measurement bias (unitless)
δ_{B_C} Characterization bias (unitless)
U_M Relative uncertainty in the measurement value of the item (Ci)
U_C Relative uncertainty in the characterization value of the item (Ci)

The total CWTS-reported isotopic activity in a DU, I_W (Ci), is expressed as the sum of the CWTS-reported activities of each measured item, $\left(A_W \pm U_W\right)$, in that DU:

$$I_W \pm U_{I_W} = \sum_a^i \left(A_W \pm U_W\right) \quad \text{Eq. (9-7)}$$

The absolute uncertainty in this total inventory value is calculated using:

$$unc_{I_W} = \sqrt{unc_{W_a}{}^2 + unc_{W_b}{}^2 + \ldots + unc_{W_i}{}^2} \quad \text{Eq. (9-8)}$$

where:

$unc_{W_a} \ldots unc_{W_i}$ Absolute uncertainty, $\left(A_W \times U_W\right)$, for each measured waste item (Ci)

Similarly, the total true isotopic activity in a DU, I_T (Ci), is expressed as the sum of the true activities of each measured item in Ci, $\left(A_T \pm U_{A_T}\right)$, in that DU:

$$I_T \pm U_{I_T} = \sum_a^i \left(A_T \pm U_{A_T}\right) \quad \text{Eq. (9-9)}$$

The absolute uncertainty in this total inventory value is calculated using:

$$unc_{I_T} = \sqrt{unc_{T_a}{}^2 + unc_{T_b}{}^2 + \ldots + unc_{T_i}{}^2} \quad \text{Eq. (9-10)}$$

where:

unc_{T_a} … unc_{T_i} Absolute uncertainty, $\left(A_T \times U_{A_T}\right)$, for each measured waste item (Ci)

These values are related through the equation:

$$I_T \pm unc_{I_T} = I_W \times \delta_B \pm unc_{I_W} \qquad \text{Eq. (9-11)}$$

where:

δ_B Total inventory bias in the DU calculated from $\left(I_T / I_W\right)$ [unitless].

The relative uncertainty in a DU, U_{DU}, is simply calculated from $\left(unc_{I_T} / I_T\right)$ or $\left(unc_{I_W} / I_W\right)$.

By normalizing I_W to 1.0 and using it as the mean and using U_{DU} as the uncertainty, a PDF and CDF can be created (e.g., see Figure 9-5). These parameters (I_W, U_{DU}, and δ_B) and its CDF are used during closure analysis.

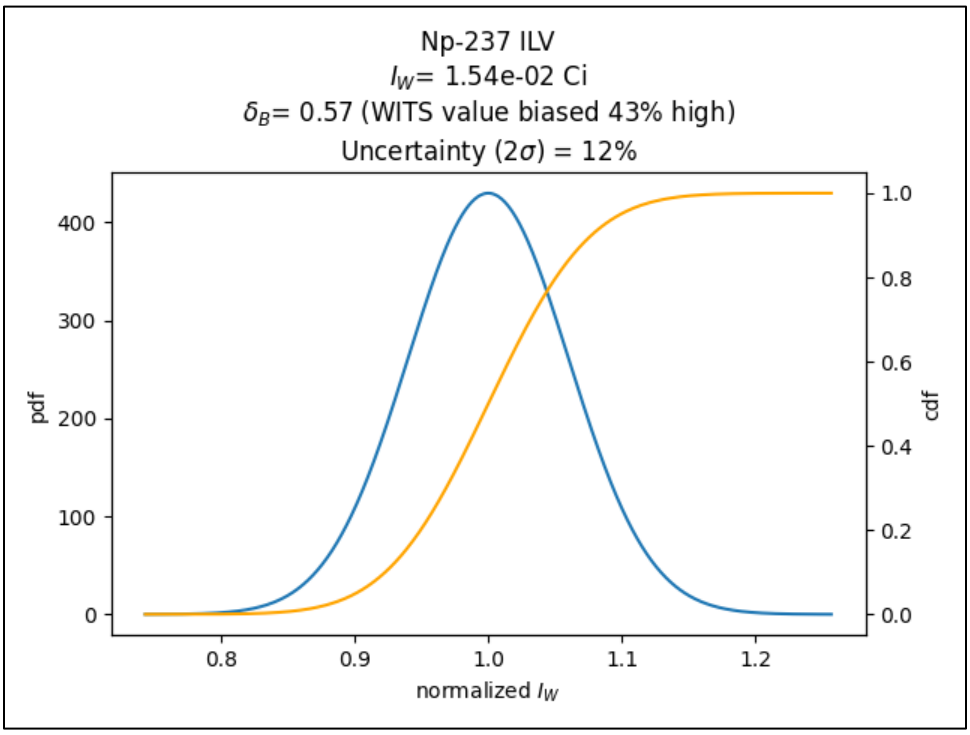

Figure 9-5. Inventory Uncertainty for Np-237 in Intermediate-Level Vault

During the closure analysis, which is a MC process, many estimated final inventories of a radionuclide in a DU are generated as discussed in Section 9.1.2.1. Each of these values is multiplied by the bias factor to get the true estimate of final DU inventory (I_T). Then, each of these true closure inventory estimates are multiplied by the normalized inventory selected from the CDF. Using Np-237 in the ILV as an example, if a random value, which must be between 0.0

and 1.0 (the *y*-axis), of 0.5 is selected, the normalized inventory of 1.0 is returned. If a random value of 0.8 is selected, a normalized inventory value of approximately 1.06 is returned. These normalized values are multiplied by I_T to get the final inventory in a DU for this MC run. For radionuclides with small uncertainty, the normalized inventory value will be close to 1.0. For a radionuclide with a large uncertainty, such as the activity of Np-237 in the average ST (Figure 9-6), this value will vary by a much larger amount. In this case, using a random value of 0.8 returns a normalized value of approximately 2.0.

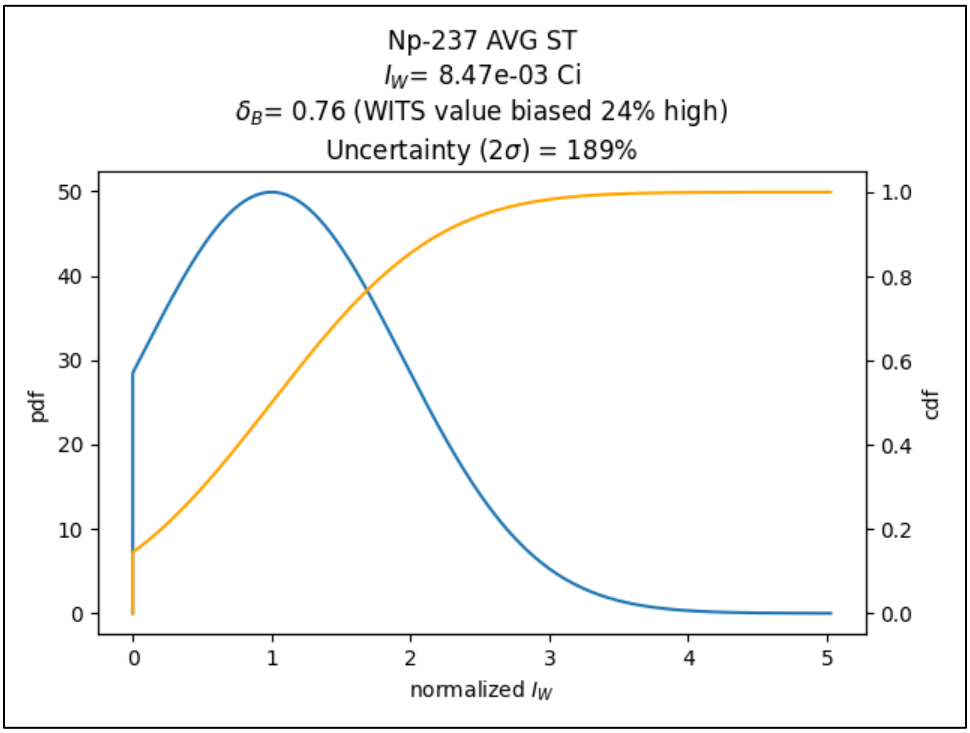

Figure 9-6. Average Inventory Uncertainty for Np-237 in Slit Trenches

The isotopic inventory uncertainty distribution and bias values are created from the values as recorded in CWTS. These are sufficient for closed DUs; however, for future DUs or DUs that are still open, additional isotopic values may be needed. Additionally, there are SWFs included in the closure analysis that are not currently labeled as such within CWTS. To ensure there are uncertainty and bias values for each generic waste form and SWF radionuclide in each DU (current and future), the following procedures are used.

First, all DUs that currently contain waste (closed and open DUs as shown in Table 9-3) are examined. For each of these DUs, uncertainty and bias files for radionuclides expected to participate in each of the four exposure pathways (GW, IHI, air, and radon as provided in Chapter 8) are verified to exist. If these radionuclide files are not found, because they do not exist in CWTS for this DU, a placeholder file is created for them. The placeholder files (bias and CDF) are created using the following values:

- I_W ~ 1.0E-12 Ci (1.0 pCi)
- U_{DU} = 10%
- δ_B = 1.0 (unbiased)

Table 9-3. Disposal Unit and Waste Acceptance Status

DU	DU Status
ST01, ST02, ST03, ST04, ST05	Closed
ST06, ST07, ST08, ST09, ST14	Open
ST10, ST11, ST18, ST24	Future
ST23 [a]	Open
ET01	Closed
ET02, ET03	Open
ET04, ET05, ET07, ET08, ET09	Future
LAWV	Open
ILV	Open
NR07E	Closed
NR26E	Open

Notes:

[a] See text below for ST23 discussion.

I_W is approximately 1.0 pCi (random value centered around 1.0E-12 Ci with a 10% standard deviation). This is done so that if these placeholder files are the only ones available for the DUs that currently exist, the average standard deviation among the inventories will not be zero (calculated for future DUs). The above approach is used for all closed and open DUs with the exception of ST23. All inventory currently disposed in ST23 as of March 31, 2021, is considered the CIG SWF, as denoted by an "A" appended to the radionuclide symbol. CWTS has not yet been updated with this information; therefore, the CIG SWF and other SWFs, such as tall boxes and welded NR casks, are addressed during the analysis. Future inventory in ST23 will be treated as using the average trench inventory as discussed for all future DUs below.

Future DUs use the average value as calculated in the following manner. For each radionuclide in a current type of DU (ST or ET), the CWTS/placeholder activity, the estimated true activity, and the absolute uncertainty of the CWTS activity are multiplied by an averaging factor and divided by the current composition vector's SOF total (see Table 9-4). These adjusted values are used to calculate the relative uncertainty and the bias factor (true activity / CWTS activity).

The parameters for future DUs are then selected using the worst-case values from the above list. For the uncertainty, the maximum value of the relative uncertainty is used. The future inventory is the arithmetic average of the activities, and the bias factor is the minimum bias factor used.

These parameters are used to create the average CDF and bias files. Future ETs use the average ET values and future STs (except ST10, which uses ST09 values) and ST23 use the average ST values to create the isotopic CDF and bias files employed in the closure analysis. Appendix I, Section I.2, contains a series of tables, one for each DU, showing the radionuclides and parameter settings used for the closure analysis.

Table 9-4. Parameters for Open Disposal Units

DU	Average Factor	SOF Total
ET01, ST01, ST02, ST03, ST04, ST05	1.00	1.000
ET02	0.95	0.751
ET03		0.352
ST06		0.143
ST07		0.456
ST08		0.370
ST09		0.936
ST14		0.943

9.1.2.4. Closure Analysis Details and Results

The base case is defined as follows:

- GWP (beta-gamma, gross-alpha, radium, and uranium) pathways; all-pathways; IHI-chronic and IHI-acute pathways; air pathway; and radon pathway are all considered active in computing inventories.
- CWTS inventory bias and uncertainty are included for all radionuclides in each DU.
- Uncertainties in 2065 projected closure inventories are included (DU closure composition).

For deterministic analyses, no uncertainties are considered while the option to apply biases is addressed. For stochastic analyses, uncertainties are incorporated while inventory biases are always being applied.

The maximum total doses and concentrations listed in Table 9-1 for the GW pathways (i.e., GWP pathways plus all-pathways) all occur along the North curtain of the 100-meter POA. As such, all deterministic and stochastic results presented in this chapter and Appendix I refer to profiles or point values along the North curtain. The hydrostratigraphy on this vertical curtain is shown in Figure 9-7 where the three sandy aquifer units and two clayey confining units are highlighted.

The individual circles in Figure 9-7 represent PORFLOW cell center locations along the vertical curtain. Sandy soils are colored coded in light brown and clayey soils are color coded in light green. The portions of the North curtain residing within the different PIF aquifer cutouts are labeled at the top of Figure 9-7 (note that there is actual overlap of aquifer cutouts, but the curtain nodes and their values remain unique). As Figure 9-7 illustrates, a nonuniform vertical grid is employed in the PORFLOW transport model where finer resolution is needed for regions where contaminant plumes will exist.

Figure 9-8 displays the water saturation profile on the North curtain during the initially uncovered time period (TP0) where node locations with values greater than 0.999 are shaded in light blue. One distinct feature of the profile is the location of the water table surface versus the location of the TCCZ. The water table drops below the TCCZ in the western regions of E-Area and along part of the center regions, while it lies above the TCCZ throughout the remainder of the center and eastern regions. A perched water table is also predicted in the eastern sector that partially extends into the western sector boundary.

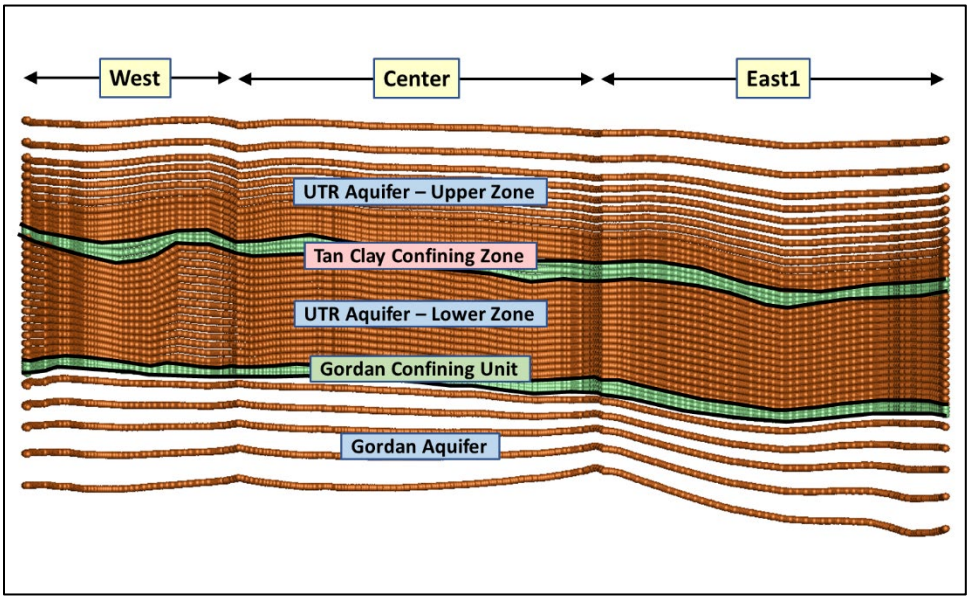

Figure 9-7. Hydrostratigraphy on North Curtain Representing 100-meter POA

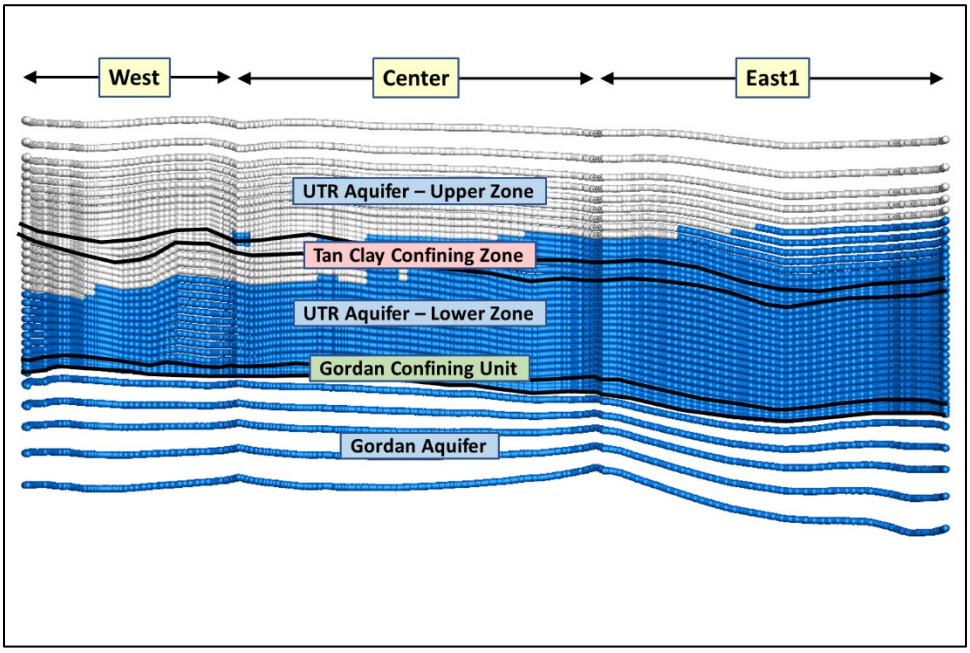

Figure 9-8. Water Saturation Profile on North Curtain Representing 100-meter POA (TP0)

For results within the compliance periods, the deterministic and stochastic analyses for the GW pathways (GWP pathways plus all-pathways) employ the above North curtain as described above. Concentrations along this North curtain are obtained from PORFLOW HIST command files and are then converted into doses where appropriate.

For assessing maximum dose and concentration profiles during the post-compliance period (i.e., beyond Year 1,171), the PORFLOW STAT command files are utilized. The STAT files have some level of conservatism built into them because they only store maximum concentrations at and

beyond the 100-meter POA. Storage limitations made the option of using HIST files unmanageable.

9.1.2.4.1. Deterministic Results Within Compliance Periods

As described in Sections 9.1.2.2 and 9.1.2.3, two separate stochastic pieces comprise the closure analysis. For deterministic analyses, the uncertainty in CWTS inventories and the uncertainty in projected DU compositions at closure are not addressed. Specifically, CWTS parent radionuclide closure inventories are only adjusted based on their individual bias factors (multipliers), which are DU dependent (see Appendix I, Section I.2, for multipliers). DU future compositions are set to their best estimate values based on ~26 years of ELLWF operations (see Appendix H, Section H.7.2, for best-estimate future composition vectors).

A single deterministic case run is made where results associated with each individual pathway and contributing parent radionuclide are stored. Graphical results for the overall facility (ELLWF) and for individual DUs are then generated. A summary of results is provided in Appendix I, Section I.4.1. Section I.4.1.1 presents dose and concentration time profiles for each of the nine exposure pathways for the ELLWF as a whole and the top-ten individual DU contributors. Section I.4.1.2 similarly provides dose and concentration time profiles for the nine exposure pathways for the 27 individual PA2022 DUs and their top-ten parent radionuclide contributors.

The SOF metric must be employed to compare results between differing pathways. Specifically, each dose or concentration is normalized by its appropriate PO criterion. Based on the deterministic aspects highlighted earlier, the resulting overall maximum total SOF history profiles (transient curves) for each pathway are shown in Figure 9-9 for a relative comparison.

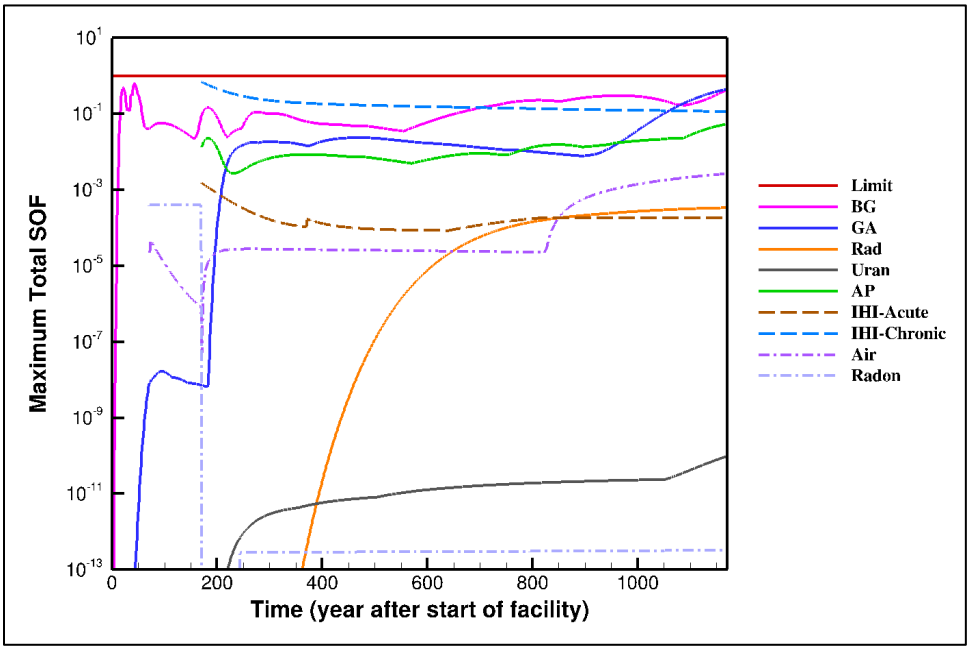

Figure 9-9. Deterministic E-Area Low-Level Waste Facility Maximum Total Sum-of-Fractions for Each Exposure Pathway

Each curve in Figure 9-9 represents the maximum total SOF on the POA (100-meter POA, within DU, or ground surface) by pathway. The results shown cover the overall compliance period that encompasses all the individual compliance periods (Years 0 to 1,171 after the start of the facility in September 1994). As expected, no PO is exceeded during this overall compliance period when the assumptions employed in the deterministic analysis remain valid.

The results in Table 9-1 represent the maximum total dose or concentration per pathway at its pathway-chosen POA. The results are based on the CWTS projected closure inventories where the bias factors are applied. Each of the doses and concentrations are converted into maximum total SOFs as listed in Table 9-5. The resulting SOFs are also rank ordered; pathways with a SOF greater than 1% are shaded in orange.

Table 9-5. Deterministic, Rank-Ordered, Maximum Total Sum-of-Fractions

Exposure Pathway	Pathway ID	Maximum Total SOF at POA (%)
IHI Chronic	IHI-Chronic	68.33%
GWP Beta-Gamma	BG	64.75%
GWP Gross-Alpha	GA	44.04%
All-Pathways	AP	5.39%
Air	Air	0.27%
IHI Acute	IHI-Acute	0.15%
Radon	Radon	0.04%
GWP Radium	Rad	0.03%
GWP Uranium	Uran	9.83E-09%

Notes:

[a] CWTS inventory bias factors applied.

To illustrate how the maximum total SOF profiles shown in Figure 9-9 are comprised of contributions from multiple DUs, as well as the parent radionuclides within these DUs, the results for the four more-limiting pathways (orange shading in Table 9-5) are discussed in greater detail in the next four subsections. Focus is placed on the most-limiting DU for each exposure pathway along with its top radionuclide contributors.

9.1.2.4.1.1. Deterministic Beta-Gamma Results

The major DU contributor to beta-gamma dose is the future slit trench, ST24 (Figure 9-10). Considering the beta-gamma GW pathway (compliance period: Years 0 to 1,171) alone, the top-ten, rank-ordered DU contributors are shown in Figure 9-10. As the righthand image (Years 0 to 100) indicates, ST24's contribution to beta-gamma dose is the largest, followed by ST01.

A comparison of the maximum total dose and SOFs for several of the more substantial DU contributors is provided in Table 9-6, which displays results for the overall ELLWF and its top-ten DU contributors. The peak concentration for each DU occurs at different locations along the North curtain and at different times within the compliance period. The maximum dose (with bias factors applied) for the ELLWF is highlighted in orange and corresponds to the beta-gamma dose listed in Table 9-1.

The total dose profile at a point in time for the ELLWF represents the arithmetic sum of the dose profiles from every DU within the ELLWF. The locations and times of the maximum total dose for each DU and for the ELLWF will in general differ.

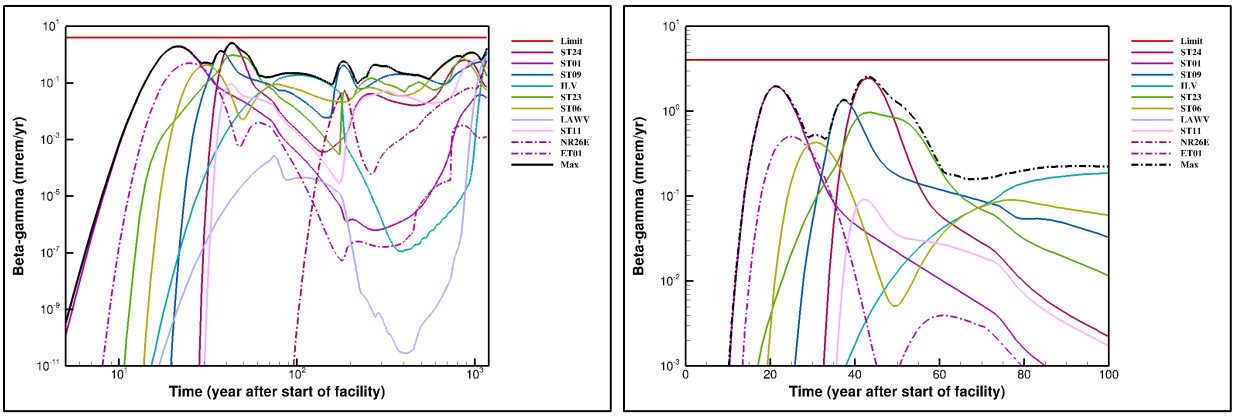

Figure 9-10. Deterministic Beta-Gamma Total Dose (Years 0 to 1,171) for ELLWF and Top-Ten Contributing Disposal Units

Table 9-6. Deterministic Beta-Gamma Total Doses and Sum-of-Fractions for ELLWF and Top-Ten Contributing Disposal Units

ELLWF/DU	Dose (mrem yr^{-1})	SOF [a] (-)	Percent of Dose vs. Maximum Dose	Time of Peak Value (Relative Year)
ELLWF	2.590	0.647	100.00%	43
ST24	2.484	0.621	95.92%	
ST01	1.981	0.495	76.49%	21
ST09	1.352	0.338	52.20%	37
ILV	1.213	0.303	46.85%	1,171
ST23	1.161	0.290	44.83%	968
ST06	0.870	0.217	33.59%	815
LAWV	0.829	0.207	31.99%	1,166
ST11	0.697	0.174	26.90%	1,059
NR26E	0.620	0.155	23.92%	1,171
ET01	0.505	0.126	19.51%	25

Notes:

The maximum dose and SOF (with bias factors applied) for the ELLWF are highlighted in orange and corresponds to the beta-gamma dose listed in Table 9-1.

[a] SOFs computed using the PO of 4 mrem yr^{-1}.

Figure 9-11 displays the ELLWF beta-gamma total dose profile on the North curtain corresponding to Year 43 (during the initially uncovered operations). The location of the overall maximum concentration (and dose) is circled and is consistent with the downstream plume emanating from ST24. The main contributor to the peak at Year 43 for ST24, and thus for ELLWF, is H-3.

The top-ten, rank-ordered parent radionuclide contributors to the total beta-gamma dose from ST24 are shown in Figure 9-12. As the righthand plot (Years 0 to 100) indicates, H-3 releases from ST24 dominate.

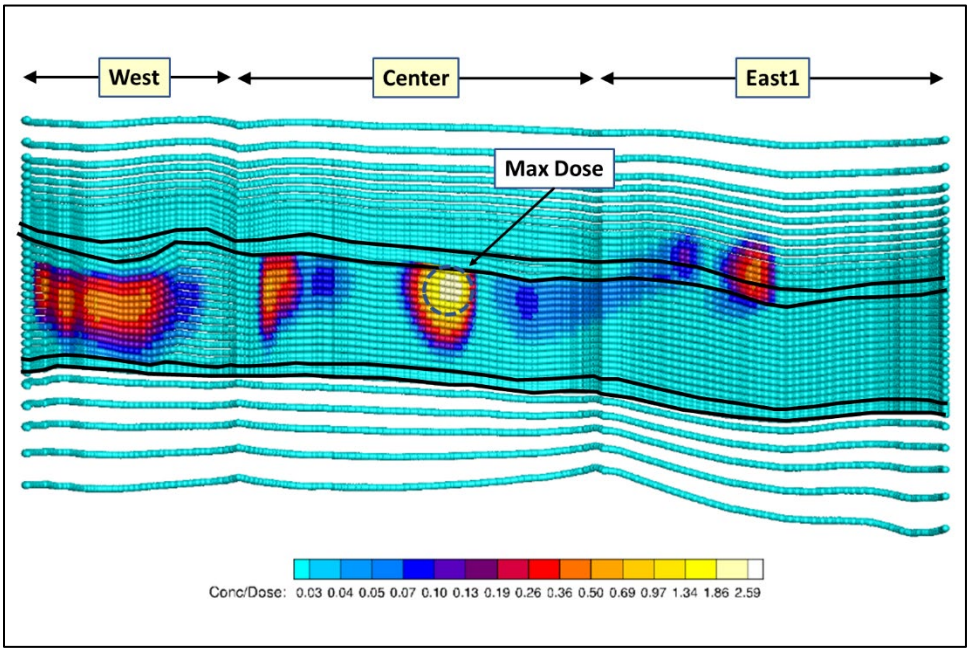

Figure 9-11. Deterministic Beta-Gamma Dose at Year 43 on North Curtain

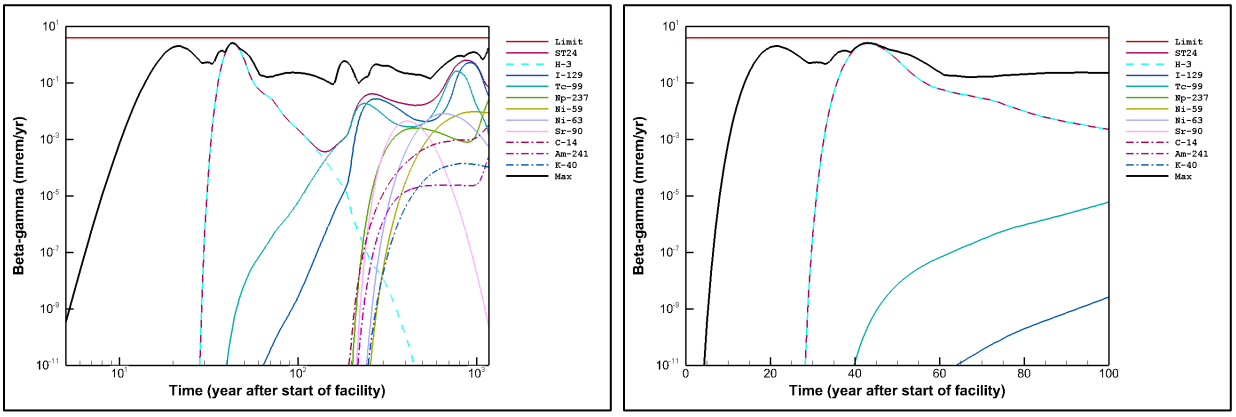

Figure 9-12. Deterministic Beta-Gamma Dose (Years 0 to 1,171) for ST24 and Top-Ten Radionuclides

This breakdown in beta-gamma total dose by top-ten contributing radionuclide for ST24 is also provided in Table 9-7. The maximum total SOF for ST24 occurs at Year 43 with a SOF equal to 0.621 (2.484 mrem yr^{-1}). H-3 represents 100.00% of ST24's total beta-gamma dose at the 100-meter POA.

Figure 9-9 as well as Figure 9-10 through Figure 9-12 present the deterministic PA results with the CWTS inventory bias factors applied. A similar set of deterministic analyses are available where the bias factors have not been applied. A comparison of results with and without application of the bias factors is provided in Table 9-8 for the beta-gamma GW pathway. The table lists the maximum dose (and SOF) for the ELLWF, ST24, and ST24's top-ten radionuclide contributors at the peak time for the ELLWF of Year 43.

Table 9-7. Deterministic Beta-Gamma Doses and Sum-of-Fractions for ST24 and Top-Ten Radionuclides

DU/Radionuclide	Dose (mrem yr^{-1})	SOF (-)	Percent of Dose vs. Maximum Dose	Time of Peak Value (Relative Year)
ST24	2.484	0.621	100.00%	43
H-3	2.484	0.621	100.00%	43
I-129	0.523	0.131	21.07%	922
Tc-99	0.262	0.065	10.54%	776
Np-237	0.026	0.006	1.03%	1,171
Ni-59	0.009	0.002	0.38%	973
Ni-63	0.008	0.002	0.33%	659
Sr-90	0.004	0.001	0.18%	410
C-14	0.003	0.001	0.13%	1,171
Am-241	0.000	0.000	0.01%	1,171
K-40	0.000	0.000	0.01%	834

Table 9-8. Deterministic Beta-Gamma Dose Sensitivity to Bias Factor for ELLWF, ST24, and H-3

ELLWF/DU/ Radionuclide	Units	Dose (SOF)		Time (Relative Year)	Bias Factor (multiplier)
		With Bias Factors Applied	Without Bias Factors Applied		
ELLWF	mrem yr^{-1}	2.590 (0.647)	2.690 (0.672)	43	--
ST24		2.484 (0.621)	2.580 (0.645)		--
H-3	% of ST24	100.00%	100.00%		0.96301

Notes:

The maximum dose and SOF (with bias factors applied) for the ELLWF are highlighted in orange and corresponds to the beta-gamma dose listed in Table 9-1.

9.1.2.4.1.2. Deterministic Gross-Alpha Results

Radionuclide contributors to gross-alpha include Ra-226 but exclude radon and uranium. The major DU contributor to gross-alpha concentration is future engineered trench, ET08 (Figure 9-13). Considering the gross-alpha GW pathway alone, the top-ten, rank-ordered DU contributors are shown in Figure 9-13. As the righthand image (Years 800 to 1,150) indicates, ET08's contribution to gross-alpha concentration is the largest, with slightly smaller contributions from its nearest neighbors ET07 and ET09.

A comparison of the maximum total concentration and SOFs for several of the more significant DU contributors is provided in Table 9-9, which displays results for the overall ELLWF and its top-ten DU contributors. The peak concentration for each DU occurs at different locations along the North curtain but at the same peak time (Year 1,171). The maximum concentration (with bias factors applied) for the ELLWF is highlighted in orange and corresponds to the gross-alpha concentration listed in Table 9-1.

The total concentration profile for the ELLWF represents the arithmetic sum of the concentration profiles for every DU within the ELLWF. The locations of the maximum total concentrations for each DU and for the ELLWF will in general differ.

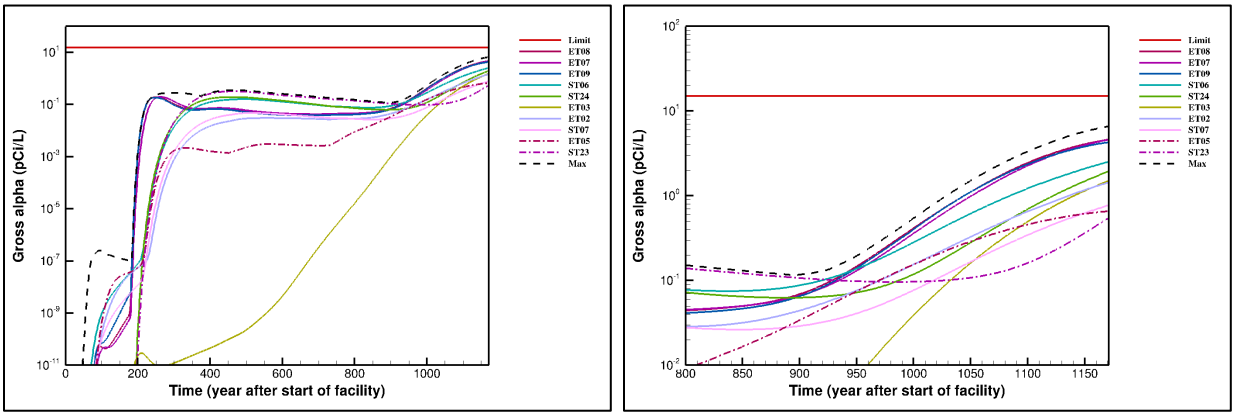

Figure 9-13. Deterministic Total Gross-Alpha Concentration (Years 0 to 1,171) for ELLWF and Top-Ten Contributing Disposal Units

Table 9-9. Deterministic Gross-Alpha Total Concentrations and Sum-of-Fractions for ELLWF and Top-Ten Contributing Disposal Units

ELLWF/DU	Concentration (pCi L^{-1})	SOF [a] (-)	Percent of Concentration vs. Maximum Concentration	Time of Peak Value (Relative Year)
ELLWF	6.606	0.440	100.00%	1,171
ET08	4.599	0.307	69.61%	
ET07	4.599	0.307	69.61%	
ET09	4.278	0.285	64.76%	
ST06	2.520	0.168	38.15%	
ST24	1.949	0.130	29.50%	
ET03	1.493	0.100	22.60%	
ET02	1.436	0.096	21.74%	
ST07	0.775	0.052	11.72%	
ET05	0.657	0.044	9.94%	
ST23	0.548	0.037	8.30%	

Notes:

The maximum concentration and SOF (with bias factors applied) for the ELLWF are highlighted in orange and corresponds to the gross-alpha concentration listed in Table 9-1.

[a] SOFs computed using the PO concentration of 15 pCi L^{-1}.

Figure 9-14 displays the ELLWF gross-alpha total concentration profile on the North curtain corresponding to Year 1,171. The location of the overall maximum concentration is circled and is consistent with the downstream plumes emanating from ET07 and ET08.

The top-ten, rank-ordered parent radionuclide contributors to gross-alpha total concentration from ET08 are shown in Figure 9-15. As the righthand plot (Years 800 to 1,150) indicates, Np-237 releases from ET08 dominate.

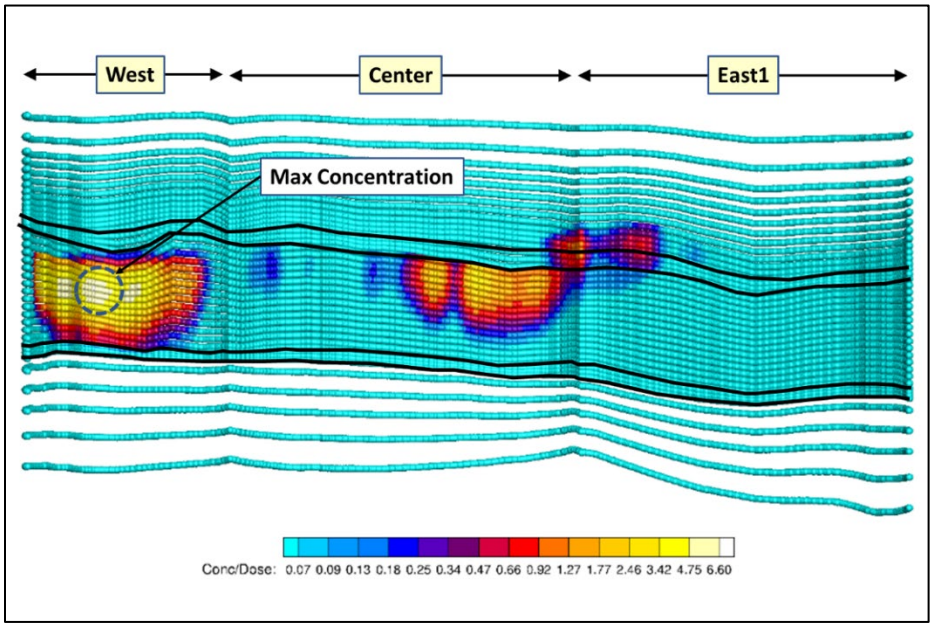

Figure 9-14. Deterministic Gross-Alpha Concentration at Year 1,171 on North Curtain

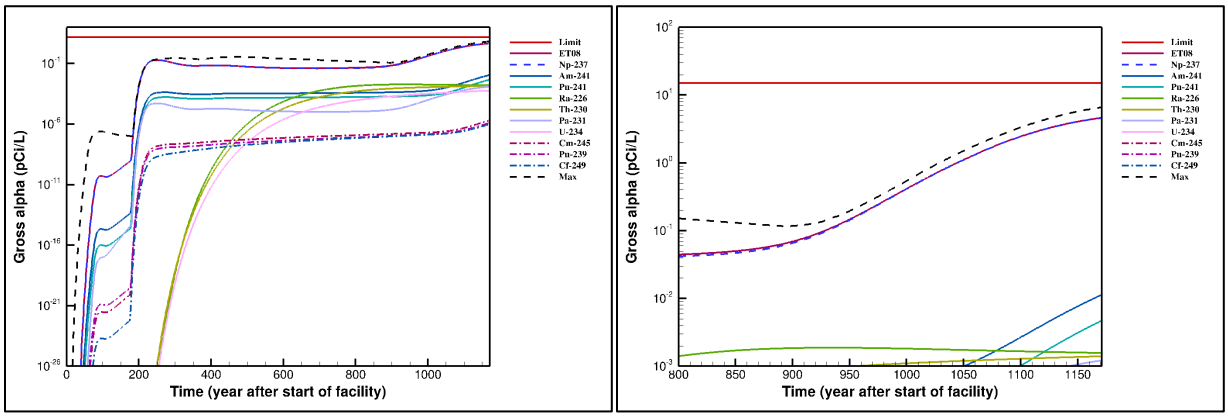

Figure 9-15. Deterministic Gross-Alpha Concentration (Years 0 to 1,171) for ET08 and Top-Ten Radionuclide Contributors

This breakdown in gross-alpha total concentration by top-ten contributing radionuclide for ET08 is also provided in Table 9-10. The maximum total SOF for ET08 occurs at Year 1,171 with a SOF equal to 0.307 (4.599 pCi L^{-1}). Np-237 represents 99.55% of the ET08's total gross-alpha concentration at the 100-meter POA.

Figure 9-9 as well as Figure 9-13 through Figure 9-15 present the deterministic results with the CWTS inventory bias factors applied. A similar set of deterministic analyses are available where the bias factors have not been applied. A comparison of the results with and without application of the bias factors is provided in Table 9-11 for the gross-alpha GW pathway. The table lists the maximum concentration (and SOF) for the ELLWF, ET08, and ET08's top-ten radionuclide contributors at the peak time for the ELLWF of Year 1,171. As shown in Table 9-11, bias factors play an important role in computed dose, while they are relatively insensitive to radionuclide rank ordering.

Table 9-10. Deterministic Gross-Alpha Concentrations and Sum-of-Fractions for ET08 and Top-Ten Radionuclide Contributors

DU/Radionuclide	Concentration ($pCi\ L^{-1}$)	SOF (-)	Percent of Maximum Concentration	Time of Peak Value (Relative Year)
ET08	4.599	0.307	100.00%	1,171
Np-237	4.578	0.305	99.55%	
Am-241	0.011	0.001	0.25%	
Pu-241	0.005	0.000	0.10%	
Ra-226	0.002		0.04%	934
Th-230	0.001		0.03%	1,171
Pa-231			0.03%	
U-234			0.01%	
Cm-245	0.000		0.00%	
Pu-239				
Cf-249				

Table 9-11. Deterministic Gross-Alpha Sensitivity to Bias Factor for ELLWF, ET08, and ET08 Top-Ten Radionuclide Contributors

ELLWF/DU/ Radionuclide	Units	Concentration (SOF)		Time (Relative Year)	Bias Factor (multiplier)
		With Bias Factors Applied	Without Bias Factors Applied		
ELLWF	$pCi\ L^{-1}$	6.606 (0.440)	10.773 (0.718)	1,171	--
ET08		4.599 (0.307)	7.500 (0.500)		--
Np-237	% of ET08	99.55%	99.58%		0.61301
Am-241		0.25%	0.25%		0.61081
Pu-241		0.10%	0.10%		0.60861
Ra-226		0.04%	0.03%		0.78766
Th-230		0.03%	0.02%		1.00000
Pa-231					1.00000
U-234		0.01%	0.01%		0.69485
Cm-245		0.00%	0.00%		0.58003
Pu-239					0.66922
Cf-249					0.54486

Notes:

The maximum concentration and SOF (with bias factors applied) for the ELLWF are highlighted in orange and corresponds to the gross-alpha concentration listed in Table 9-1.

9.1.2.4.1.3. Deterministic All-Pathways Results

The major DU contributor to all-pathways is the future engineered trench, ET07 (Figure 9-16). Considering the all-pathways GW pathway (compliance period: Years 171 to 1,171) alone, the top-ten, rank-ordered DU contributors are shown in Figure 9-16. As the righthand image (Years 800 to 1,150) indicates, ET07's contribution to all-pathways dose is the largest, with slightly smaller contributions from its nearest neighbors, ET08 and ET09.

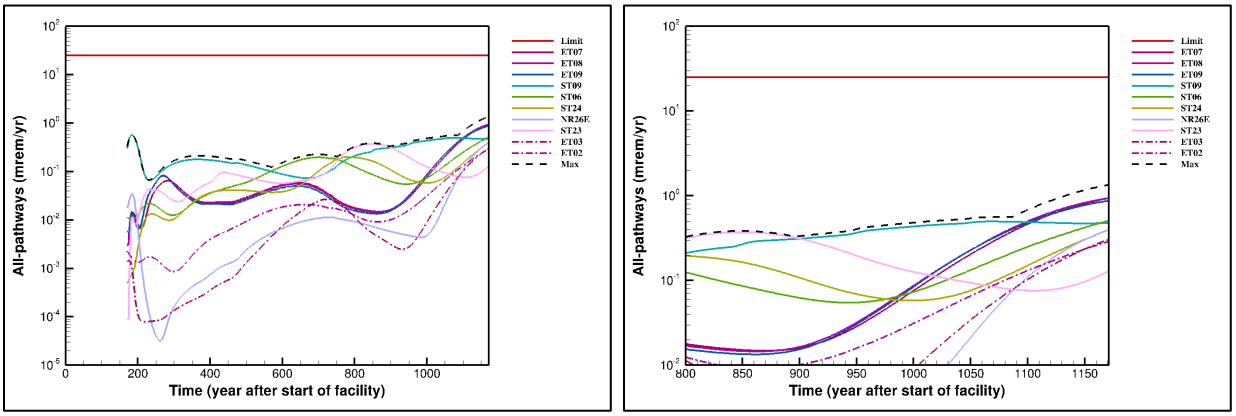

Figure 9-16. Deterministic All-Pathways Total Dose (Years 171 to 1,171) for Top-Ten Disposal Unit Contributors

A comparison of the maximum total dose and SOFs for several of the more substantial DU contributors is provided in Table 9-12, which displays results for the overall ELLWF and its top-ten DU contributors. The peak dose for each DU occurs at different locations along the North curtain but at the same peak time (Year 1,171). The maximum dose (with bias factors applied) for the ELLWF is highlighted in orange and corresponds to the all-pathways dose listed in Table 9-1.

Table 9-12. Deterministic All-Pathways Total Doses and Sum-of-Fractions for ELLWF and Top-Ten Disposal Unit Contributors

ELLWF/DU	Dose (mrem yr^{-1})	SOF [a] (-)	Percent of Dose vs. Maximum Dose	Time of Peak Value (Relative Year)
ELLWF	1.347	0.0539	100.00%	1,171
ET07	0.938	0.0375	69.59%	
ET08	0.937	0.0375	69.56%	
ET09	0.872	0.0349	64.71%	
ST09	0.570	0.0228	42.32%	184
ST06	0.508	0.0203	37.69%	1,171
ST24	0.397	0.0159	29.48%	
NR26E	0.395	0.0158	29.33%	
ST23	0.372	0.0149	27.58%	849
ET03	0.305	0.0122	22.65%	1,171
ET02	0.288	0.0115	21.41%	

Notes:

The maximum dose and SOF (with bias factors applied) for the ELLWF are highlighted in orange and corresponds to the all-pathways dose listed in Table 9-1.

[a] SOFs computed using the PO dose of 25 mrem yr^{-1}.

The total dose profile for the ELLWF represents the arithmetic sum of the dose profiles from every DU within the ELLWF. The locations of the maximum total dose for each DU and for the ELLWF will in general differ.

The all-pathways total dose profile on the North curtain for the ELLWF at Year 1,171 is shown in Figure 9-17. The location of the overall maximum dose is circled and is consistent with the downstream plumes emanating from ET07 and ET08.

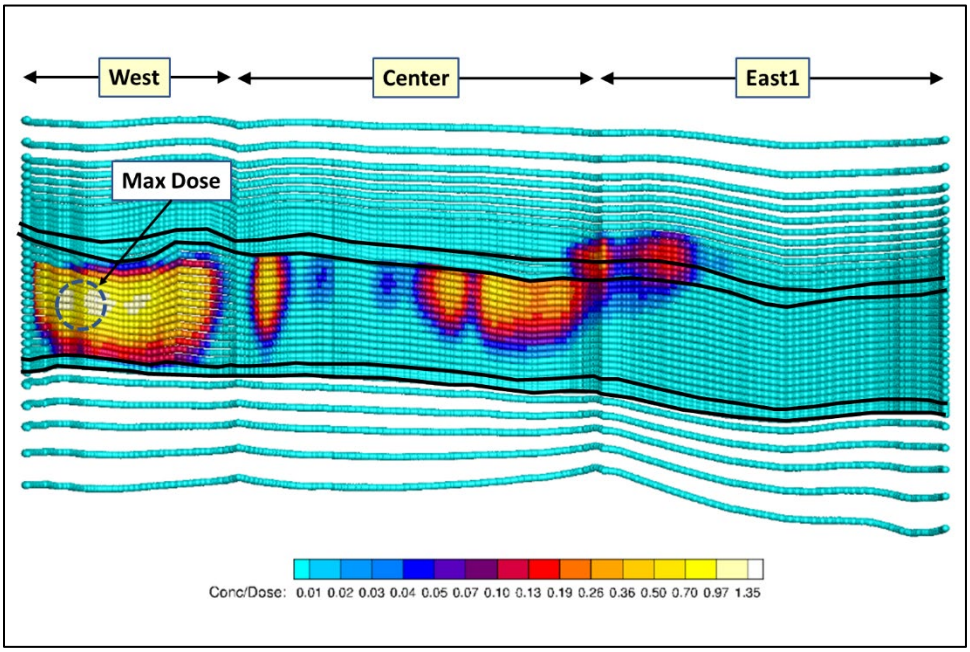

Figure 9-17. Deterministic All-Pathways Dose at Year 1,171 on North Curtain

The top-ten, rank-ordered parent radionuclide contributors to the all-pathways total dose from ET07 are shown in Figure 9-18. As the righthand plot (Years 800 to 1,150) indicates, Np-237 releases from ET07 dominate.

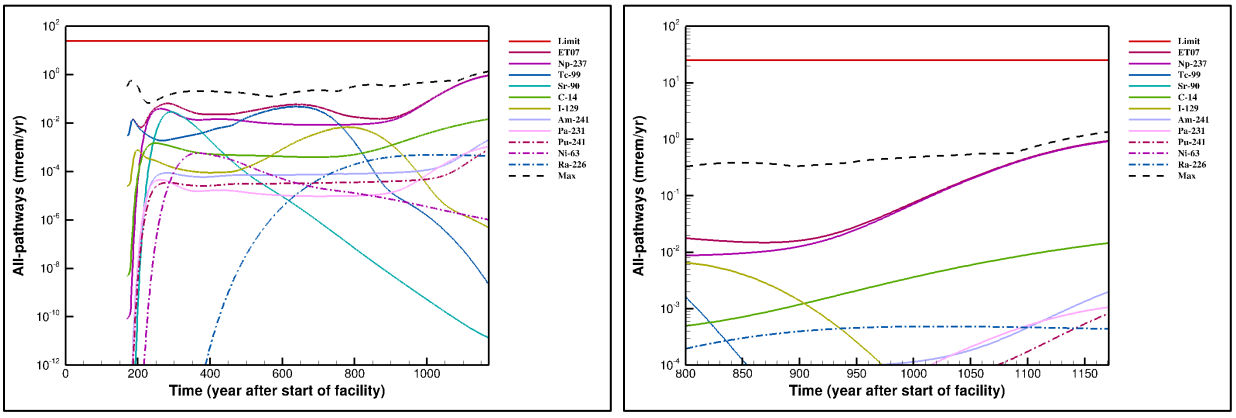

Figure 9-18. Deterministic All-Pathways Dose (Years 171 to 1,171) for ET07 and Top-Ten Radionuclide Contributors

The top-five parent radionuclide contributors to all-pathways total dose are listed in Table 9-13. The maximum total SOF for ET07 occurs at Year 1,171 with a SOF equal to 0.0375 (0.938 mrem yr^{-1}). Np-237 represents 97.94% of ET07's total all-pathways dose at the 100-meter POA.

Table 9-13. Deterministic All-Pathways Doses and Sum-of-Fractions for ET07 and Top Radionuclide Contributors

DU/Radionuclide	Dose (mrem yr^{-1})	SOF (-)	Percent of Dose vs. Maximum Dose	Time of Peak Value (Relative Year)
ET07	0.938	0.0375	100.00%	1,171
Np-237	0.918	0.0367	97.94%	
C-14	0.014	0.0006	1.54%	
Am-241	0.002	0.0001	0.22%	
Pa-231	0.001	0.0000	0.11%	
Pu-241			0.09%	

Figure 9-9 as well as Figure 9-16 through Figure 9-18 display the deterministic results with the CWTS inventory bias factors applied. A similar set of deterministic analyses are available where the bias factors have not been applied. A comparison of the results with and without application of the bias factors is provided in Table 9-14 for the all-pathways GW pathway. The table lists the maximum dose (and SOF) for the ELLWF, ET07, and ET07's top radionuclide contributors.

Table 9-14. Deterministic All-Pathways Dose Sensitivity to Bias Factor for ELLWF, ET07, and ET07 Top Radionuclide Contributors

ELLWF/DU/ Radionuclide	Units	Dose (SOF)		Time (Relative Year)	Bias Factor (multiplier)
		With Bias Factors Applied	Without Bias Factors Applied		
ELLWF	mrem yr^{-1}	1.347 (0.0539)	2.184 (0.0874)	1,171	--
ET07		0.938 (0.0375)	1.520 (0.0608)		--
Np-237	% of ET07	97.94%	98.55%		0.61301
Tc-99		5.12%	4.65%	636	0.67887
Sr-90		3.09%	2.79%	292	0.68344
C-14		1.54%	1.00%	1,171	0.95630
I-129		0.72%	0.68%	780	0.64865
Am-241		0.22%	0.22%	1,171	0.61081
Pa-231		0.11%	0.09%		1.00000
Pu-241		0.09%	0.07%		0.60861
Ra-226		0.05%	0.04%	1,020	0.78766

Notes:

The maximum dose and SOF (with bias factors applied) for the ELLWF are highlighted in orange and corresponds to the all-pathways dose listed in Table 9-1.

9.1.2.4.1.4. Deterministic IHI-Chronic Results

The major DU contributor to IHI-Chronic total dose is the open NRCDA, NR26E (Figure 9-19). Considering the IHI-Chronic pathway (compliance period: Years 171 to 1,171) alone, the top-ten, rank-ordered DU contributors are shown in Figure 9-19, with NR26E contributing the largest dose. The POA for the acute and chronic IHI pathways is an individual DU. No plume interaction applies between neighboring DUs; therefore, doses are associated with each DU separately.

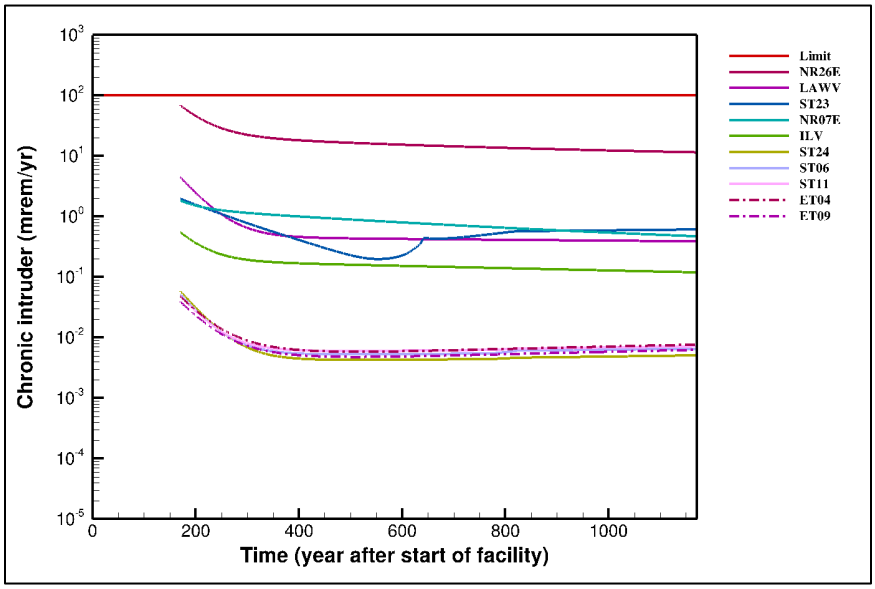

Figure 9-19. Deterministic IHI-Chronic Total Dose (Years 171 to 1,171) for Top-Ten Disposal Unit Contributors

A comparison of the maximum total dose and SOFs for the top-ten largest DU contributors is provided in Table 9-15. The peak IHI-Chronic dose occurs at the start of its compliance period (Year 171) for each DU. The maximum dose and SOF shown for the ELLWF with bias factors applied corresponds to the IHI-Chronic dose listed in Table 9-1 and represents the value for NR26E.

Table 9-15. Deterministic IHI-Chronic Total Doses and Sum-of-Fractions for ELLWF and Top-Ten Contributing Disposal Units

ELLWF/DU	Dose (mrem yr^{-1})	SOF [a] (-)	Percent of Dose vs. Maximum Dose	Time of Peak Value (Relative Year)
ELLWF	68.33	0.6833	100.00%	171
NR26E	68.33	0.6833	100.00%	
LAWV	4.44	0.0444	6.49%	
ST23	1.95	0.0195	2.86%	
NR07E	1.83	0.0183	2.67%	
ILV	0.54	0.0054	0.80%	
ST24	0.06	0.0006	0.09%	
ST06	0.05	0.0005	0.08%	
ST11			0.07%	
ET04				
ET09	0.04	0.0004	0.06%	

Notes:

The maximum dose and SOF (with bias factors applied) for the ELLWF are highlighted in orange and corresponds to the IHI-Chronic dose listed in Table 9-1.

[a] SOFs computed using the PO dose of 100 mrem yr^{-1}.

The top-ten, rank-ordered parent radionuclide contributors to the IHI-Chronic total dose from NR26E are shown in Figure 9-20. As the righthand plot (Years 150 to 400) indicates, Sr-90S is the largest contributor at Year 171.

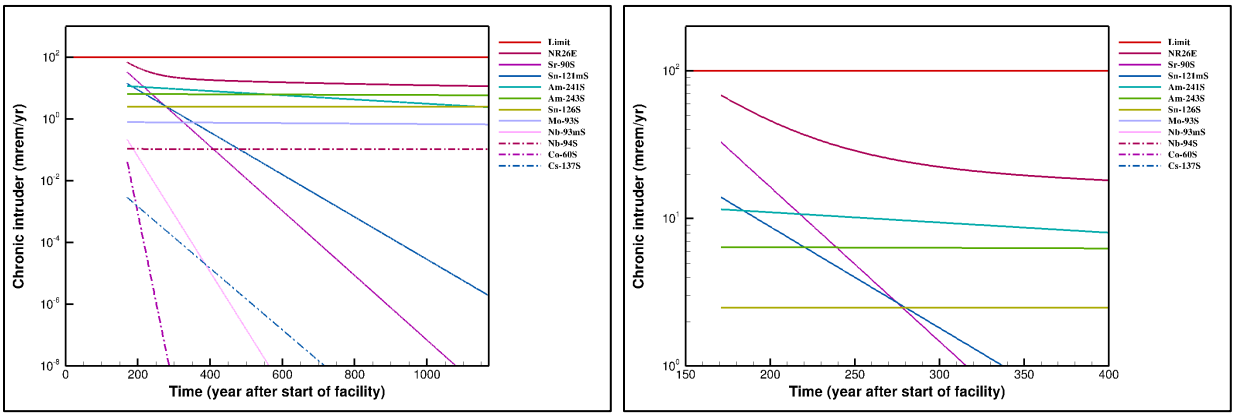

Figure 9-20. Deterministic IHI-Chronic Dose (Years 171 to 1,171) for NR26E and Top-Ten Radionuclide Contributors

A breakdown of IHI-Chronic total dose from NR26E by top-ten radionuclide contributor is also provided in Table 9-16. The maximum total SOF for NR26E occurs at Year 171 with a SOF equal to 0.6833 (68.33 mrem yr^{-1}). Sr-90S accounts for 48.13% of NR26E's total IHI-Chronic dose.

Table 9-16. Deterministic IHI-Chronic Doses and Sum-of-Fractions for NR26E and Top-Ten Radionuclide Contributors

DU/Radionuclide	Dose (mrem yr^{-1})	SOF (-)	Percent of Dose vs. Maximum Dose	Time of Peak Value (Relative Year)
NR26E	68.33	0.6833	100.00%	171
Sr-90S	32.89	0.3289	48.13%	
Sn-121mS	13.90	0.1390	20.34%	
Am-241S	11.52	0.1152	16.86%	
Am-243S	6.40	0.0640	9.36%	
Sn-126S	2.48	0.0248	3.63%	
Mo-93S	0.79	0.0079	1.15%	
Nb-93mS	0.21	0.0021	0.31%	
Nb-94S [a]	0.11	0.0011	0.16%	
Co-60S [a]	0.04	0.0004	0.06%	
Cs-137S [a]	0.00	0.0000	0.00%	

Notes:

The maximum dose and SOF (with bias factors applied) for the ELLWF are highlighted in orange and corresponds to the IHI-Chronic dose listed in Table 9-1.

[a] Special gamma ray calculations are employed that include self-shielding using the MCNP code (Verst, 2021a).

As Table 9-16 indicates, the computed dose contributions from the last three radionuclides do address gamma ray self-shielding, while the top-seven radionuclide contributors are based on standard IHI calculations. If MCNP calculations are used for the top-seven radionuclides, the maximum total SOF for NR26E will drop significantly.

Figure 9-9, Figure 9-19, and Figure 9-20 display the deterministic results with the CWTS inventory bias factors applied. A similar set of deterministic analyses are available where the bias factors have not been applied. A comparison of the results with and without application of the bias factors is provided in Table 9-17 for the IHI-Chronic pathway. The table lists the maximum dose (and SOF) for the ELLWF, NR26E, and NR26E's top radionuclide contributors. Because the bias factors for all radionuclides considered in NR26E are set to 1.0, no change in results is observed.

Table 9-17. Deterministic IHI-Chronic Dose Sensitivity to Bias Factor for ELLWF, NR26E, and NR26E Top Radionuclide Contributors

ELLWF/DU/ Radionuclide	Units	Dose (SOF)		Time (Relative Year)	Bias Factor (multiplier)
		With Bias Factors Applied	Without Bias Factors Applied		
ELLWF	mrem yr^{-1}	68.33 (0.6833)	No change	171	1.00000
NR26E		68.33 (0.6833)			
Sr-90S	% of NR26E	32.89 (0.3289)			
Sn-121mS		13.90 (0.1390)			
Am-241S		11.52 (0.1152)			
Am-243S		6.40 (0.0640)			

Notes:

The maximum dose and SOF (with bias factors applied) for the ELLWF are highlighted in orange and corresponds to the IHI-Chronic dose listed in Table 9-1.

9.1.2.4.2. Deterministic Groundwater Results for Post-Compliance Period

Section 9.1.2.4.1 summarizes deterministic analysis results within the compliance periods for a select few pathways and DUs. This section reports the results of deterministic analyses during the post-compliance period. PORFLOW transport simulations were made such that peak doses and concentrations for every parent radionuclide within every DU are observed (except for STs and ETs where a limit of 10,000 years beyond the end of IC is imposed). Only results associated with the GW pathways are considered here.

For every case (DU and parent radionuclide combination), a PORFLOW "STAT.out" file is created where the maximum radionuclide concentrations (parent and short-chain progeny) are stored at every time step. The stored values at each time step are maximum concentrations (gmol ft^{-3} per gmole parent) computed based on the region "at and beyond" the 100-meter POA. The parent and short-chain progeny concentrations are converted to activities and then expanded to full-chain progeny activities assuming secular equilibrium. The full-chain progeny activities are converted to dose factors (concentration or dose per Ci of parent) for each GW pathway and summed to each parent radionuclide. The dose factors, along with the CWTS-adjusted closure inventories, are used to compute dose history time profiles for each GW pathway.

Dose history time profiles for the GW pathways are created for each DU using (1) dose factors computed without PIFs and (2) projected CWTS closure inventories with biases applied. PORFLOW STAT files are used in lieu of HIST files during the post-compliance period because of the large memory requirements to store dose factors derived from HIST files. The resulting dose/concentration profiles of top contributing radionuclides for the GW pathways for each DU are provided in Appendix I, Section I.4.1.3.

9.1.2.4.2.1. Beta-Gamma Pathway

Figure 9-21 displays the deterministic dose profiles for the beta-gamma GW pathway until Year 10,171. Both the PO and the end of the compliance period (Year 1,171) are shown as black dashed and solid lines, respectively. The left image in Figure 9-21 shows all 27 DUs; in all cases, beta-gamma dose lies below the PO during the compliance period (to left of solid black line). However, during the post-compliance period, five DUs display a beta-gamma dose that exceeds the PO (right image in Figure 9-21).

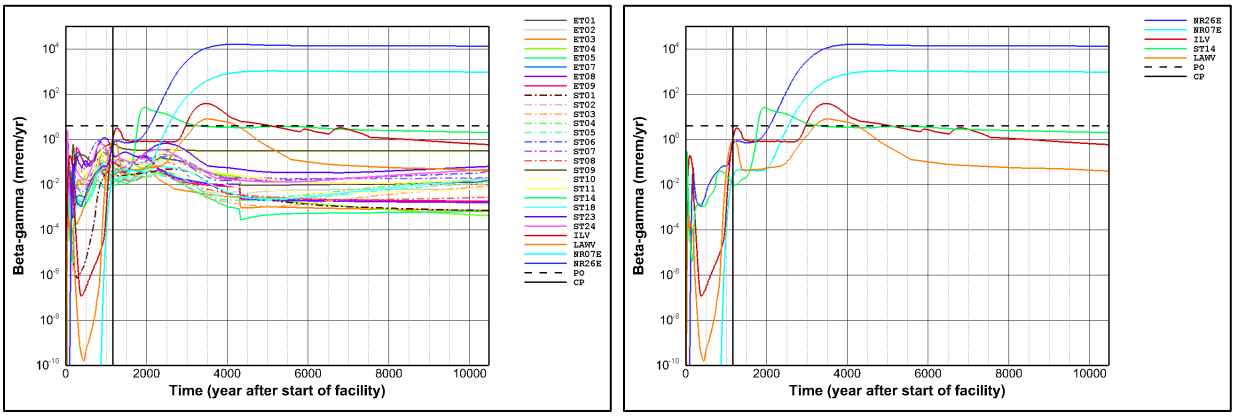

Figure 9-21. Deterministic Beta-Gamma Total Dose During Post-Compliance Period for Disposal Units

Table 9-18 compares the maximum total doses for the five DUs that exceed the PO during the post-compliance period.

Table 9-18. Deterministic Beta-Gamma Total Doses for Disposal Units Exceeding Performance Objectives During Post-Compliance Period

DU	Dose (mrem yr^{-1})	SOF [a] (-)	Time of Peak Value (Relative Year)
NR26E	16,106	4,027	4,198
NR07E	1,069	267	5,082
ILV	39	10	3,476
ST14	26	6	1,946
LAWV	8	2	3,506

Notes:

[a] SOFs computed using PO dose of 4 mrem yr^{-1}.

For NR26E, a ranking of parent radionuclide contributions to beta-gamma total dose yields the top-ten radionuclide contributors shown in Figure 9-22. The right image includes only those parent radionuclides whose dose exceeds the PO during the post-compliance period (i.e., Ni-59S and C-14S). Only parent radionuclides from SWFs have members that exceed the PO. The SWF radionuclides Ni-59S and C-14S (i.e., neutron activation products within the welded steel casks that are surface-corrosion limited) significantly exceed the PO beginning roughly 2,200 years after the end of the compliance period (i.e., Year ~3,400).

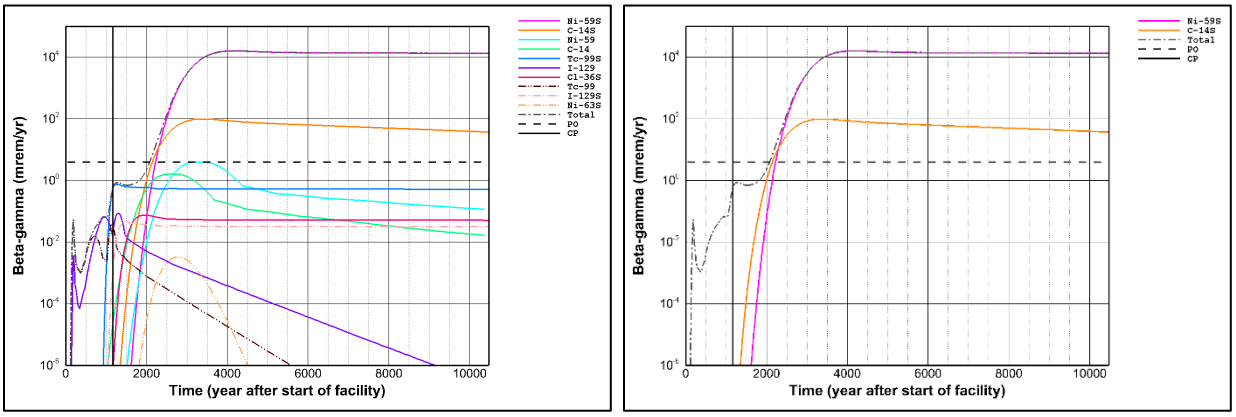

Figure 9-22. Deterministic Beta-Gamma Doses During Post-Compliance Period for NR26E and Top-Ten Radionuclide Contributors

For NR07E, a ranking of parent radionuclide contributions to beta-gamma total dose yields the top-ten contributors shown in Figure 9-23. The right image includes only those parent radionuclides whose dose exceeds the PO during the post-compliance period (i.e., Ni-59S and C-14S). The SWF radionuclides Ni-59S and C-14S (i.e., neutron activation products within the welded steel casks that are surface-corrosion limited) significantly exceed the PO beginning roughly 3,000 years after the end of the compliance period (i.e., Year ~4,200).

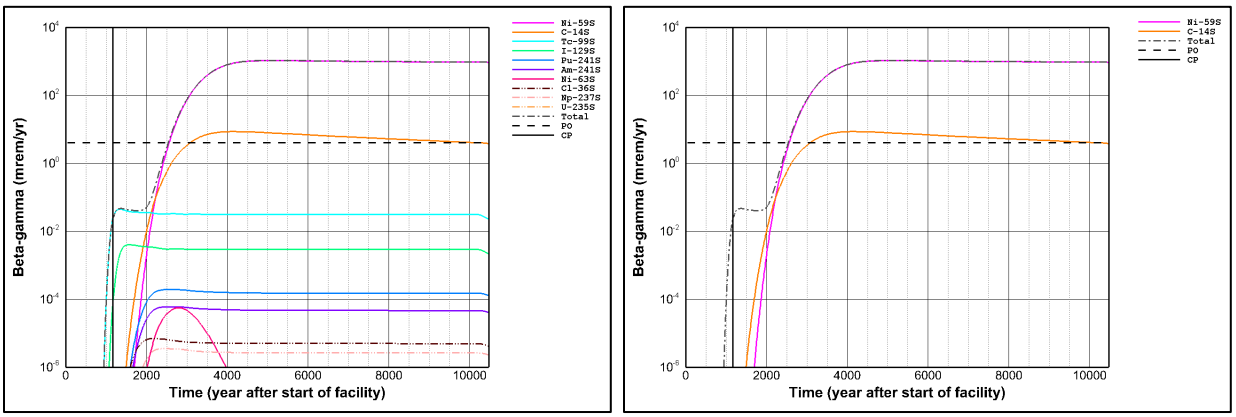

Figure 9-23. Deterministic Beta-Gamma Doses During Post-Compliance Period for NR07E and Top-Ten Radionuclide Contributors

For the ILV, a ranking of parent radionuclide contributions to beta-gamma total dose yields the top-ten radionuclide contributors displayed in Figure 9-24. The right image includes only those parent radionuclides whose dose exceeds the PO during the post-compliance period (i.e., C-14K). The largest contributor is the SWF radionuclide C-14K (K- and L-Basin Resin) with dose peaking at Year 3,466 (Table 9-18).

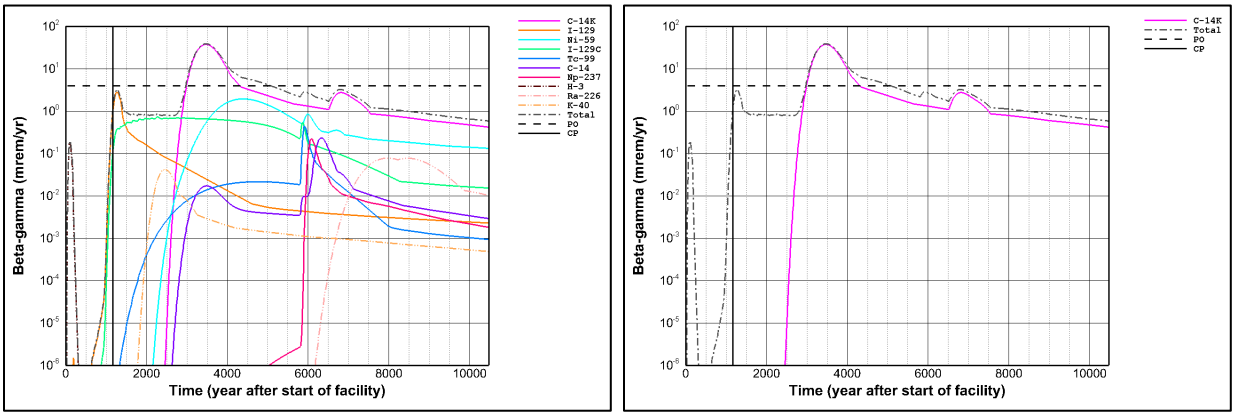

Figure 9-24. Deterministic Beta-Gamma Doses During Post-Compliance Period for ILV and Top-Ten Radionuclide Contributors

Figure 9-25 shows the top-ten radionuclide contributors to beta-gamma total dose for ST14. The right image includes the only parent radionuclide (i.e., Ni-59H) whose dose exceeds the PO, which occurs in Year 1,946 (Table 9-18). Three parent radionuclides (i.e., C-14H, Ni-59H, and Ni-63H) associated with the HWCTR SWF are top-ten contributors. The three are neutron activation products (reactor internals) that are surface-corrosion limited and begin their release into the VZ once welds associated with the blind flanges are pitted through.

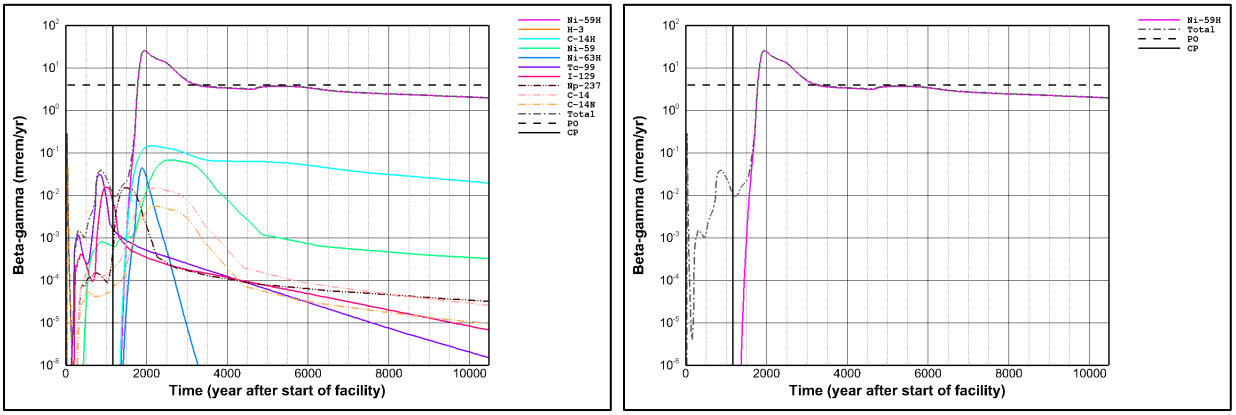

Figure 9-25. Deterministic Beta-Gamma Doses During Post-Compliance Period for ST14 and Top-Ten Radionuclide Contributors

Figure 9-26 displays the top-ten radionuclide contributors to the beta-gamma total dose for the LAWV. The right image includes the only parent radionuclide (i.e., Ni-59) whose dose exceeds the PO during the post-compliance period, which occurs in Year 3,506 (Table 9-18).

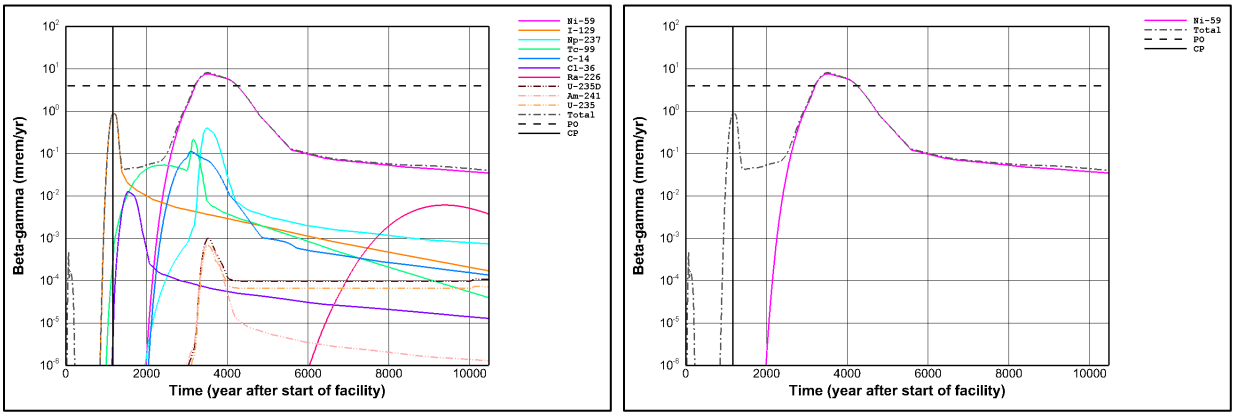

Figure 9-26. Deterministic Beta-Gamma Doses During Post-Compliance Period for LAWV and Top-Ten Radionuclide Contributors

9.1.2.4.2.2. Gross-Alpha Pathway

Figure 9-27 displays the deterministic maximum total concentrations for the gross-alpha GW pathway for a duration of 10,000 years beyond the end of IC. Both the PO and the end of the compliance period are shown as black dashed and solid lines, respectively. The left image in Figure 9-27 includes all 27 DUs and shows that DU concentrations do not exceed the PO during the compliance period. However, gross-alpha concentrations from two DUs (i.e., LAWV and ILV) exceed the PO during the post-compliance period as highlighted in the right image in Figure 9-27.

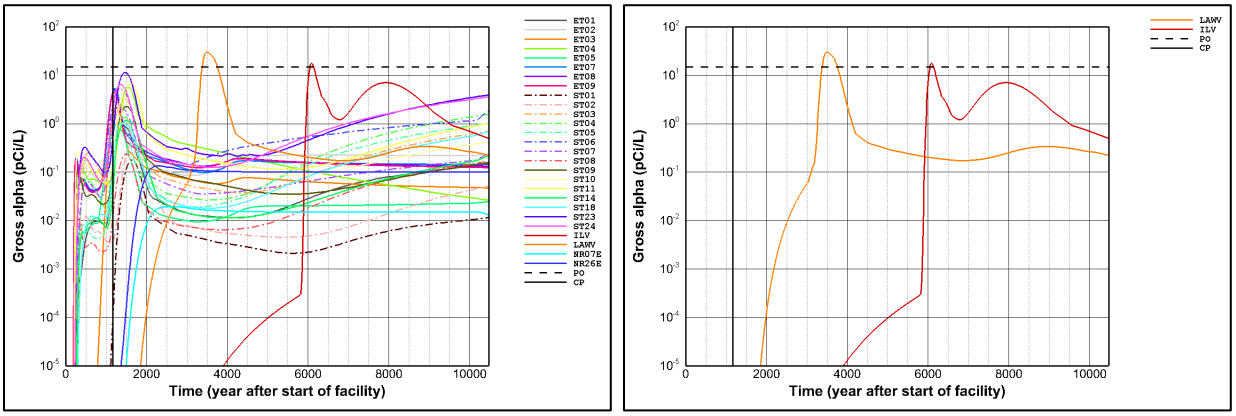

Figure 9-27. Deterministic Gross Alpha Total Concentrations During Post-Compliance Period for All Disposal Units

Table 9-19 provides a comparison of the maximum total gross-alpha concentrations and SOFs for those DUs that exceed the PO during the post-compliance period. In general, the dominant contributor to total gross-alpha concentration is Np-237.

Table 9-19. Deterministic Gross-Alpha Concentrations for Disposal Units Exceeding Performance Objectives During Post-Compliance Period

DU	Concentration (pCi L^{-1})	SOF [a] (-)	Time of Peak Value (Relative Year)
LAWV	30.5	2.0	3,496
ILV	17.7	1.2	6,086

Notes:

[a] SOFs computed using the PO concentration of 15 pCi L^{-1}.

9.1.2.4.2.3. All-Pathways

Figure 9-28 shows the deterministic maximum total doses for all-pathways for a duration of 10,000 years beyond the end of IC. Both the PO and the end of the compliance period are shown as black dashed and solid lines, respectively. The left image in Figure 9-28 includes all 27 DUs and shows that DU concentrations do not exceed the PO during the compliance period. However, all-pathways doses for two DUs (i.e., NR26E and ILV) exceed the PO during the post-compliance period as highlighted in the right image in Figure 9-28.

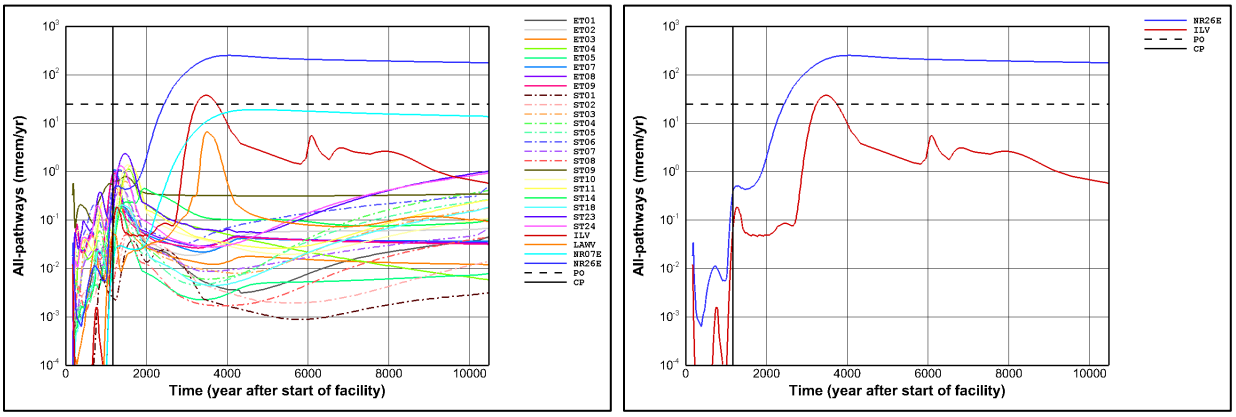

Figure 9-28. Deterministic All-Pathways Total Doses During Post-Compliance Period for All Disposal Units

Table 9-20 provides a comparison of the maximum total all-pathways dose and SOFs for those DUs that exceed the PO during the post-compliance period.

Table 9-20. Deterministic All-Pathways Doses for Disposal Units Exceeding Performance Objectives During Post-Compliance Period

DU	Dose (mrem yr^{-1})	SOF [a] (-)	Time of Peak Value (Relative Year)
NR26E	251.6	10.1	4,047
ILV	37.9	1.5	3,466

Notes:

[a] SOFs computed using the PO dose value of 25 mrem yr^{-1}.

9.1.2.4.2.4. IHI-Chronic Pathway

For the IHI-Chronic pathway analyses, no release of radionuclides is assumed to occur from the waste zones due to GW leaching and volatilization into the local air space. Waste can only be

removed through excavation or agricultural activities. Radioactive decay and ingrowth of progeny occurs during the 100-year IC period (prior to IHI activities) when the waste zone is assumed to be isolated.

Figure 9-29 displays deterministic maximum total doses for the IHI-Chronic pathway for all DUs during the compliance period (Years 171 to 1,171). Based on these results and how the waste zone release mechanisms are modeled, increased doses will be minimal and are not expected to exceed the PO during the post-compliance period (i.e., until Year 10,171). Because no changes in the release mechanisms occur during the post-compliance period, the dose rate curves shown in Figure 9-29 indicate that ingrowth should not result in significant increases to Year 10,171.

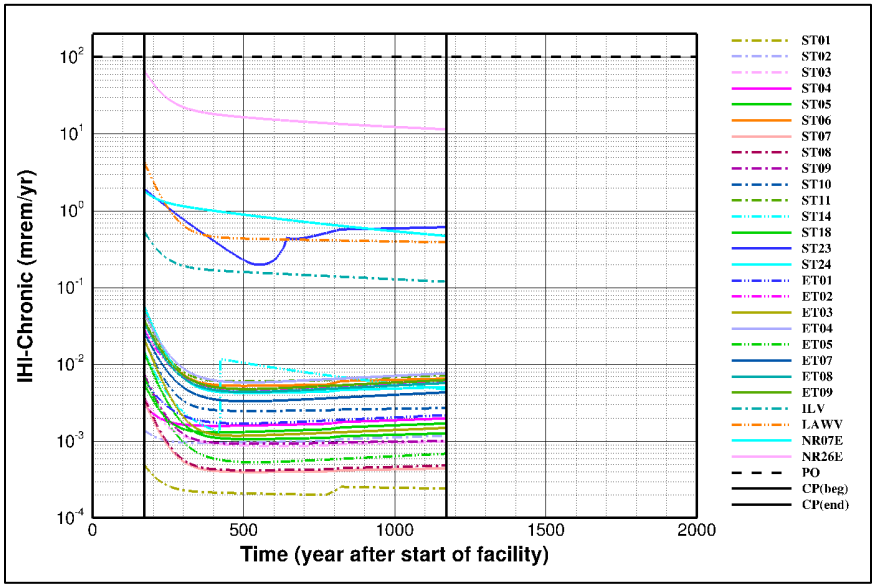

Figure 9-29. Deterministic IHI-Chronic Total Doses Within the Compliance and Post-Compliance Periods for All Disposal Units

9.1.2.4.2.5. IHI-Acute Pathway

The same modeling assumptions outlined for the IHI-Chronic pathway in Section 9.1.2.4.2.4 apply to the IHI-Acute pathway as well. Figure 9-30 displays deterministic maximum total doses for the IHI-Acute pathway for all DUs during the compliance period (Years 171 to 1,171). Based on these results and how the waste zone release mechanisms are modeled, increased doses will be minimal and are not expected to exceed the PO during the post-compliance period (i.e., until Year 10,171). Because no changes in the release mechanisms occur during the post-compliance period, the dose rate curves shown in Figure 9-30 indicate that ingrowth should not result in significant increases to Year 10,171.

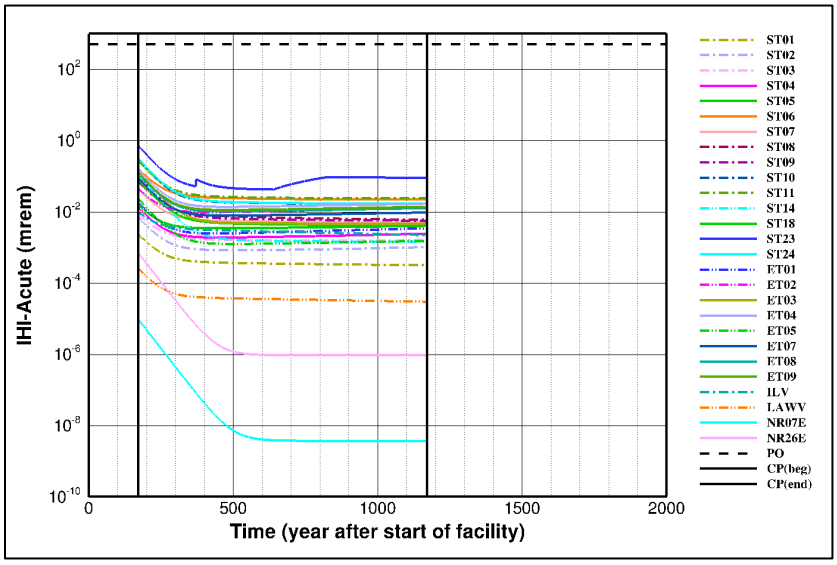

Figure 9-30. Deterministic IHI-Acute Total Doses Within the Compliance and Post-Compliance Periods for All Disposal Units

9.1.2.4.2.6. Air Pathway

The air pathway analyses assume that radionuclide release from waste zones will not occur because of GW leaching and excavation activities but only through volatilization. Two POAs are considered with nonoverlapping compliance periods (i.e., the site boundary and the 100-meter POA). The most limiting POA is DU dependent.

Figure 9-31 presents the deterministic maximum total doses for the air pathway for all DUs during the compliance (Years 71 to 1,171) and post-compliance periods (i.e., until Year 10,171). Because no changes in release mechanisms occur during the post-compliance period, the dose curves shown in Figure 9-31 indicate that ingrowth should not result in significant increases beyond Year 10,171.

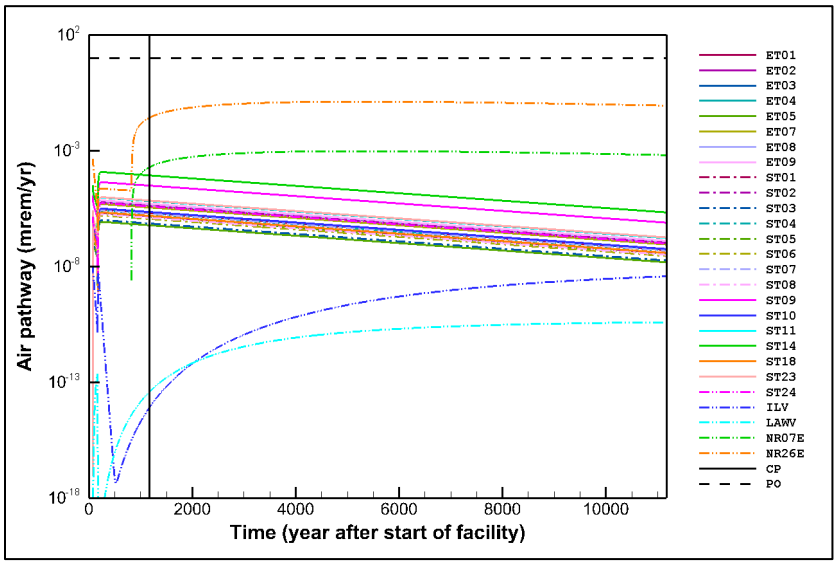

Figure 9-31. Deterministic Total Doses for Air Pathway Within the Compliance and Post-Compliance Periods

9.1.2.4.2.7. Radon Pathway

The radon pathway analyses assume that radionuclide release from waste zones will not occur because of GW leaching and excavation activities but only through volatilization and subsequent migration vertically to the ground surface. The POA is at the ground surface just above each DU's footprint; lateral spreading of the subsurface plumes is assumed to be negligible.

Figure 9-32 presents the deterministic maximum total doses for the radon pathway for all DUs during the compliance (Years 71 to 1,171) and post-compliance periods (i.e, until Year 10,171). Because no changes in the release mechanisms occur during the post-compliance period, the dose curves shown in Figure 9-32 indicate that ingrowth should not result in significant increases beyond Year 10,171.

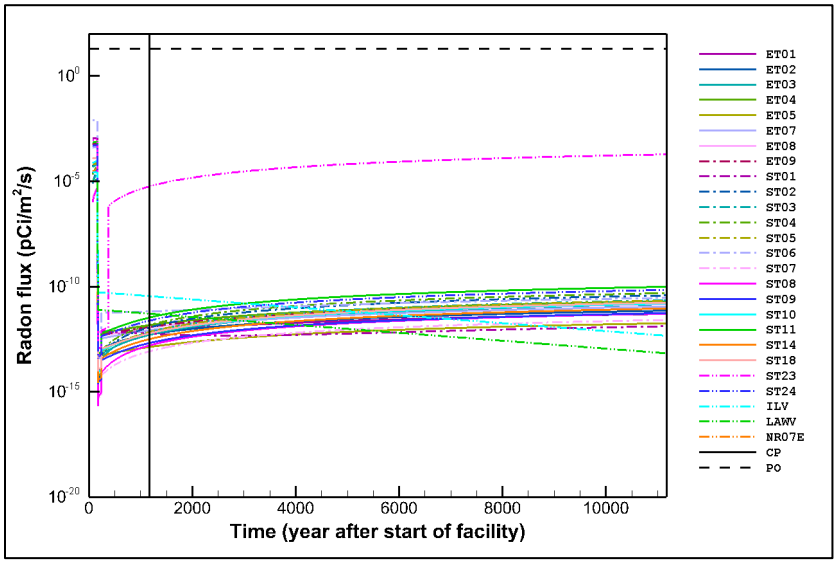

Figure 9-32. Deterministic Fluxes for Radon Pathway Within the Compliance and Post-Compliance Periods

9.1.2.4.3. Stochastic Results Within Compliance Periods

As introduced in Section 9.1.1.1, a stochastic dose/concentration analysis is conducted using the MC simulation method and is limited to time periods within the compliance periods. The results presented below and in Appendix I are based on 10,000 MC realizations that have been determined to yield reasonably accurate statistics for the low probability event of primary interest (i.e., exceedance of a SOF of 1.0, which implies exceedance of a PO).

The stochastic analysis explicitly addresses generic waste form and SWF parent radionuclides requiring inventory limits for all 27 PA2022 DUs. Dose impacts associated with a parent radionuclide's progeny are implicitly handled through dose factors. All nine exposure pathways (i.e., beta-gamma, gross-alpha, radium, uranium, all-pathways, IHI-Chronic, IHI-Acute, air, and radon), including time windows associated with certain GW pathways, are considered. GW PIFs are not explicitly employed for the GW pathways because the aquifer concentration profiles extracted from the PORFLOW transport runs (history files) are used to arrive at total concentrations along the 100-meter POA (accounts for DU plume overlap). For the air pathway, a

single air PIF (η^{Air} = 27) equal to the number of existing and future DUs is used directly in computing inventory limits for each DU.

The deterministic results in Section 9.1.2.4.1 address "nominal behavior" of the dose and concentration time histories only; no explicit accounting for CWTS radionuclide inventory uncertainties and projected closure DU composition uncertainties are considered. However, these two sources of uncertainty are included in the stochastic closure analysis results below.

The stochastic closure analysis finds that the likelihood of exceeding an absolute SOF of 1.0 is acceptably small (i.e., exceedance probability of < 3%) within the appropriate compliance periods when operating within the new ELLWF's CWTS inventory limits (i.e., values provided in Chapter 8 and Appendix H).

9.1.2.4.3.1. Peak Dose (or Concentration) Calculational Method

A curtain of 33,360 elements (834 West to East x 40 vertical elements) constitutes the 100-meter POA northern boundary (North curtain) that intercepts the GW flow trajectories of the 27 DUs (STs, ETs, LAWV, ILV, NR07E, and NR26E). The purpose of the curtain is to superimpose the concentration and dose contributions from each of the ELLWF radionuclides in the 27 DUs. This superposition of concentrations and doses is possible because of the linearity of the advection-dispersion transport equation. The curtain is a way to rigorously account for plume interaction from each DU for the GW pathways.

The following method illuminates the spatial and timing dose contributions from each DU:[2]

$$EPOA\%GWPW(ii,j) = \sum_{u=1}^{nEDU} DU(u)\%GWPW(i,j) \qquad \text{Eq. (9-12)}$$

where:

EPOA	GW transient total dose or concentration along North curtain of 100-meter POA
GWPW(ii,j)	GW pathway (GWPB, GWPA, GWPR, GWPU, or PAAP)[3] history concentrations and doses
DU(u)	ST01-ST11, ST14, ST18, ST23, ST24, ET01-ET05, ET07-ET09, LAWV, ILV, NR07E, and NR26E
ii	Global element index (1 to 33,600)
i	Local element index (aquifer cutout dependent)
j	Time index (Years 0 to 1,171)
u	Disposal unit index (1 to 27)
nEDU	Number of ELLWF DUs

[2] The % in Eq. (9-12) implies that variables belong to a Fortran-derived data type or structure.
[3] GWPB (GWP beta-gamma); GWPA (GWP gross-alpha); GWPR (GWP radium); GWPU (GWP uranium); PAAP (PA all-pathways).

The GW transient total DU dose/concentration on the local aquifer cutouts is expressed as follows:

$$DU(u)\%GWPW(i,j) = \sum_{n=1}^{nGW} DU(u)\%gNUC(n)\%GWPW_{DF}(i,j) \times (DU(u)\%gNUC(n)\%Inv_{old} + DU(u)\%gNUC(n)\%Inv_{new}) \quad \text{Eq. (9-13)}$$

where:

$gNUC(n)$	List of GW parent radionuclides in *DU*
$GWPW_{DF}(i,j)$	GW pathway history dose/concentration factors
Inv_{old}	Existing inventory of parent radionuclide in *DU* (Ci)
Inv_{new}	Future inventory of parent radionuclide in *DU* (Ci)
n	Radionuclide index (1 to *nGW*)
nGW	Number of GW parent radionuclides in *DU*

IHI transient doses are computed for each DU similarly to the GW pathways but without any spatial variation:

$$DU(u)\%PAII(j) = \sum_{n=1}^{nIHI} DU(u)\%iNUC(n)\%PAII_{DF}(j) \times (DU(u)\%iNUC(n)\%Inv_{old} + DU(u)\%iNUC(n)\%Inv_{new}) \quad \text{Eq. (9-14)}$$

where:

$iNUC(n)$	List of IHI parent radionuclides in *DU*
$PAII(j)$	Acute or chronic IHI transient doses (mrem or mrem yr^{-1}, respectively)
$PAII_{DF}(j)$	Acute or chronic IHI transient dose factors (mrem Ci^{-1} or mrem yr^{-1} Ci^{-1})
$nIHI$	Number of IHI parent radionuclides in *DU*

Air pathway transient doses are computed for each DU as follows:

$$DU(u)\%AIRP(j) = \sum_{n=1}^{nAIR} DU(u)\%aNUC(n)\%AIRP_{DF}(j) \times (DU(u)\%aNUC(n)\%Inv_{old} + DU(u)\%aNUC(n)\%Inv_{new}) \quad \text{Eq. (9-15)}$$

where:

$aNUC(n)$	List of air pathway parent radionuclides in *DU*
$AIRP(j)$	Air pathway transient doses (mrem yr^{-1})
$AIRP_{DF}(j)$	Air pathway transient dose factors (mrem yr^{-1} Ci^{-1})
$nAIR$	Number of air pathway parent radionuclides in *DU*

For the air pathway, the North curtain is a single node where complete overlap of all 27 DU plumes is assumed. The contribution of air pathway transient doses from each DU is computed for the ELLWF as follows:

$$ELLWF\%AIRP(j) = \sum_{u=1}^{nEDU} DU(u)\%AIRP(j) \quad \text{Eq. (9-16)}$$

where:

ELLWF Air pathway transient total doses at 100-meter POA

Radon pathway transient fluxes are computed for each DU as follows:

$$DU(u)\%RFLX(j) = \sum_{n=1}^{nRFX} DU(u)\%rNUC(n)\%RFLX_{DF}(j) \times (DU(u)\%rNUC(n)\%Inv_{old} + DU(u)\%rNUC(n)\%Inv_{new}) \quad \text{Eq. (9-17)}$$

where:

rNUC(n) List of radon pathway parent radionuclides in *DU*
RFLX(j) Radon pathway transient fluxes (pCi m^{-2} s^{-1})
$RFLX_{DF}(j)$ Radon pathway transient flux factors (pCi m^{-2} s^{-1})
nRFX Number of radon pathway parent radionuclides in *DU*

The spatial aspects vary per exposure pathway (specifically, the number of spatial nodes considered) as follows:

- The 2-D North curtain along the 100-meter POA is represented for the GW pathways by a vector of PORFLOW elements, where plume overlap is accounted for through the summation of dose/concentration impacts from every DU. Impacts of plume overlap due to distributed sources within a given DU are directly handled during each isolated DU PORFLOW analysis. Note that each DU resides within one of the various limits aquifer cutouts as discussed in Appendix C, Section C.1.3.
- For the air pathway, the conservative (pessimistic) assumption that all DU atmospheric doses coincide (maximum values) at the same point on the 100-meter POA results in a single point.
- For both the IHI and radon pathways, the POs are assessed within the DU or at the ground surface, respectively, without any plume interaction from neighboring DUs.

Thus, for the non-GW pathways, the number of nodes reduce to just a single location per DU.

Eq. (9-13), Eq. (9-14), Eq. (9-15), and Eq. (9-17) provide the dose (or concentration) impacts at the POAs for individual parent radionuclides and for the entire DU, respectively. Eq. (9-12) and Eq. (9-16) represent the maximum total dose (or concentration) for the entire ELLWF for the GW pathways and air pathway, respectively.

The summations in Eq. (9-14), Eq. (9-15), and Eq. (9-17) for non-GW pathways reduce to the single DU with a vector of transient values that includes the peak value. The element location

where a peak occurs for the ELLWF for the GW pathways does not necessarily coincide with any of the element locations where a peak occurs for a DU.

For each MC realization, the inventories of all parent radionuclides within all DUs are first established. With these inventories, dose and concentrations are computed for individual parent radionuclides within every DU followed by summation at the DU level. Search algorithms are then used to locate peak values for rank ordering parent radionuclide and DU contributions.

9.1.2.4.3.2. Maximum Total Sum-of-Fractions Histograms

The SOF method is utilized (dose or concentration divided by its appropriate PO criterion) to compare results between differing exposure pathways. The calculational aspects employed in computing maximum total SOFs per pathway and an overall ELLWF SOF for each MC realization are consistent with the discussion in Appendix H, Section H.8. The SOFs per realization are tabulated and stored for both the overall ELLWF and individual DUs. All the resulting SOFs are documented in Appendix I, Section I.4.2, in the form of sequential MC simulation results (Section I.4.2.3), histogram plots [or bars charts] (Section I.4.2.4), and overall statistics tables (Section I.4.2.5).

To illustrate the typical sequential MC simulation results stored, SOFs for the ELLWF for all nine exposure pathways are displayed in Figure 9-33 for the final 1,000 realizations of a 10,000-realization MC simulation. Graphically, the relative mean and spread in maximum total SOFs can be seen for each pathway. For this case, the spread in gross-alpha SOFs exceeds the spread in beta-gamma SOFs. The highest maximum total SOF observed for the ELLWF during the 10,000-realization MC simulations is ~1.96.

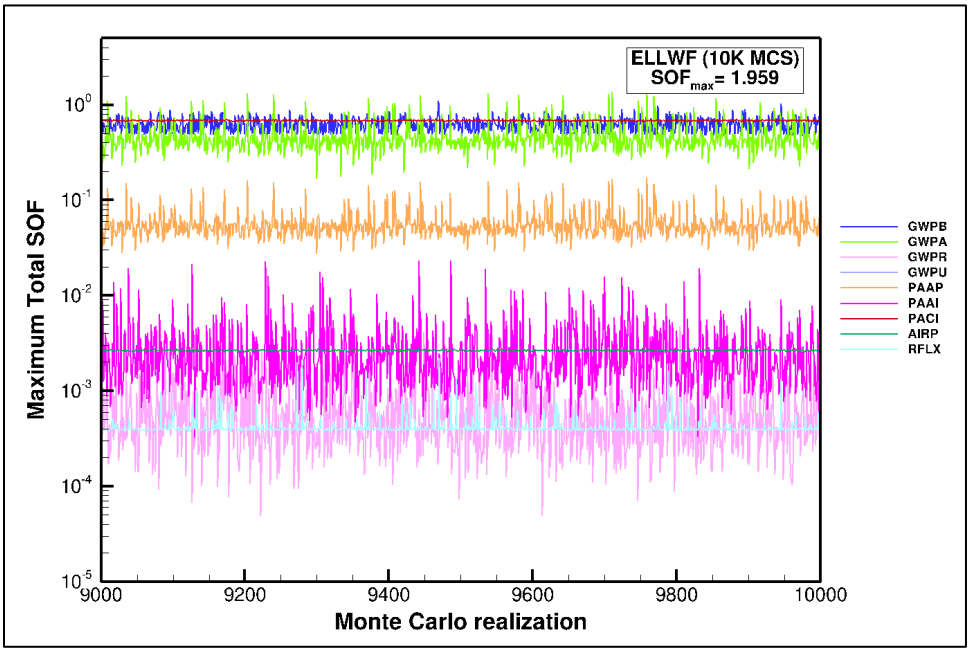

GWPB (GWP beta-gamma); GWPA (GWP gross-alpha); GWPR (GWP radium); GWPU (GWP uranium); PAAP (PA all-pathways); PAAI (PA IHI-Acute); PACI (PA IHI-Chronic); AIRP (air pathway); RFLX (radon flux)

Figure 9-33. Stochastic ELLWF Maximum Total Sum-of-Fractions for Each Exposure Pathway

Similar graphs for all 27 DUs included in the PA2022 assessment, as well as graphs displaying the total SOF for each CWTS time window in a DU, are provided in Appendix I, Section I.4.2.3.

Figure 9-34 presents the conditional probability curve for maximum total SOF for the ELLWF using a frequency plot (histogram). All results fall within the compliance periods.

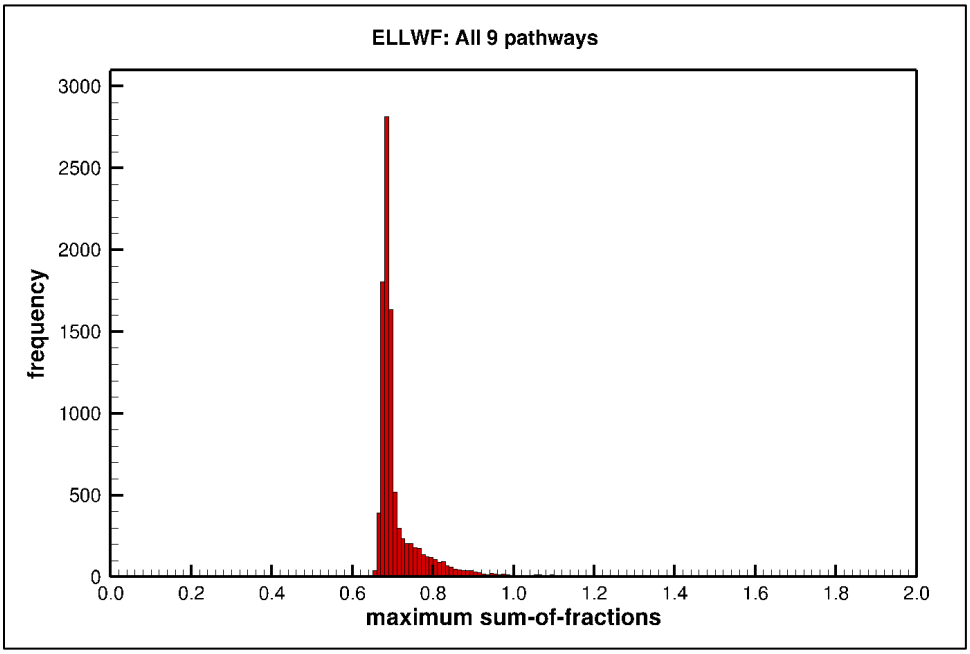

Figure 9-34. Stochastic Overall Maximum Total Sum-of-Fractions Histogram for ELLWF (10,000 Monte Carlo Realizations)

The mean value of the maximum total SOF for the ELLWF is 0.69 with an exceedance probability of 2.9% (Figure 9-1). Similar ELLWF histograms are available for all nine exposure pathways in Appendix I, Section I.4.2.4. Figure 9-35 displays the histogram plots for the beta-gamma (left) and gross-alpha (right) GW pathways.

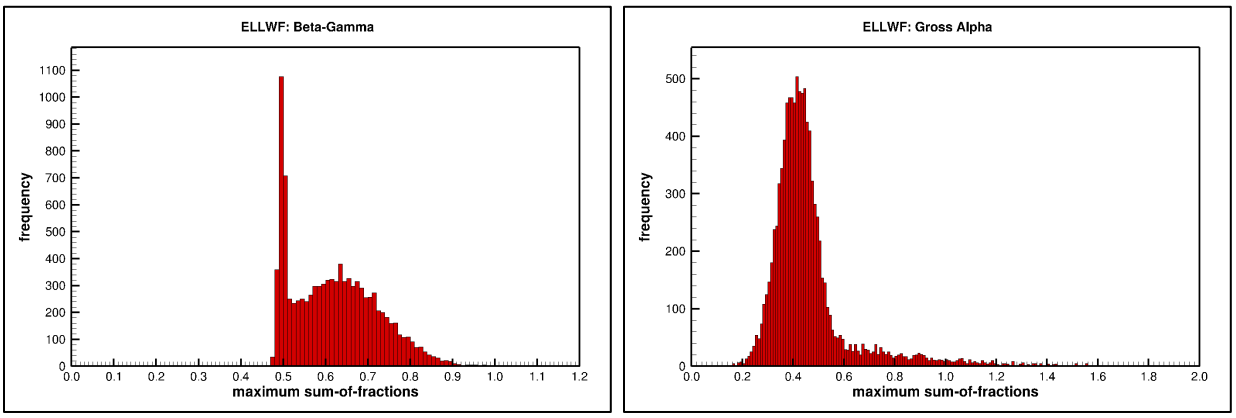

Figure 9-35. Stochastic Beta-Gamma and Gross-Alpha Maximum Total Sum-of-Fractions Histograms for ELLWF

Comparing Figure 9-34 and Figure 9-35, the shape of the ELLWF histogram is dominated by the beta-gamma GW pathway results. The stochastic behavior of individual DUs can also be observed in the histogram plots. For example, Figure 9-36 displays the maximum total SOF histogram plots for ST23 (left) and ET08 (right).

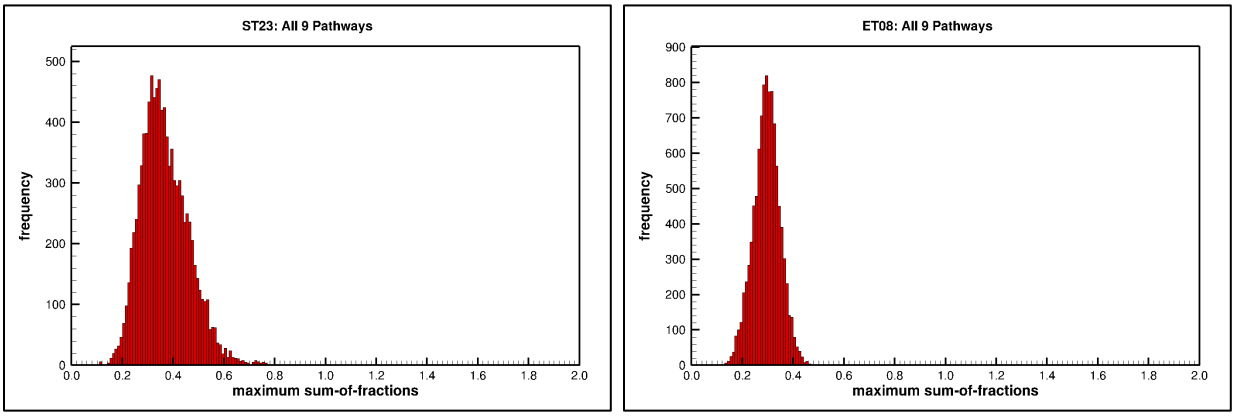

Figure 9-36. Stochastic Overall Maximum Total Sum-of-Fractions Histograms for ST23 and ET08

For several DUs and specific pathways, the mean computed SOF is quite small. Only cases where the mean computed SOF exceeds 0.1 are presented in Appendix I, Section I.4.2.4.

Statistics extracted from histogram data for every DU and exposure pathway are reported in Appendix I, Section I.4.2.5. The three key statistics computed from the data retrieved from the 10,000-realization MC simulations are the arithmetic mean, standard deviation, and coefficient of variation (standard deviation divided by mean) of the maximum total SOFs. Table 9-21 presents the summary statistics for the ELLWF, ST23, and ET08.

Table 9-21. Stochastic Maximum Total Sum-of-Fractions Statistics for ELLWF, ST23, and ET08

SOF	ELLWF			ST23			ET08		
	mean	sdev	cvar	mean	sdev	cvar	mean	sdev	cvar
Max	7.25E-01	1.06E-01	1.46E-01	3.68E-01	9.88E-02	2.68E-01	2.95E-01	5.23E-02	1.77E-01
GWPB	6.20E-01	1.02E-01	1.65E-01	3.64E-01	9.31E-02	2.55E-01	1.72E-01	9.46E-02	5.51E-01
GWPA	4.66E-01	1.81E-01	3.89E-01	6.24E-02	9.31E-02	1.49E+00	2.56E-01	9.23E-02	3.60E-01
GWPR	6.65E-04	7.78E-04	1.17E+00	6.33E-07	1.62E-06	2.56E+00	3.27E-04	5.36E-04	1.64E+00
GWPU	1.23E-10	6.74E-11	5.46E-01	4.55E-11	6.76E-11	1.49E+00	5.89E-11	2.13E-11	3.61E-01
PAAP	5.72E-02	2.16E-02	3.78E-01	1.86E-02	1.22E-02	6.56E-01	3.16E-02	1.11E-02	3.51E-01
PAAI	3.01E-03	2.95E-03	9.82E-01	2.19E-03	2.86E-03	1.30E+00	3.08E-04	3.31E-04	1.07E+00
PACI	6.84E-01	9.12E-03	1.33E-02	2.00E-02	3.49E-03	1.74E-01	4.14E-04	2.99E-04	7.22E-01
AIRP	2.66E-03	4.16E-05	1.56E-02	1.32E-06	1.29E-06	9.78E-01	8.17E-07	7.63E-07	9.34E-01
RFLX	4.40E-04	2.81E-04	6.40E-01	8.39E-05	2.47E-04	2.95E+00	4.05E-05	8.67E-05	2.14E+00

Notes:

Statistics parameters are (1) arithmetic mean (mean); (2) standard deviation (sdev); (3) coefficient of variation (cvar).

GWPB (GWP beta-gamma); GWPA (GWP gross-alpha); GWPR (GWP radium); GWPU (GWP uranium); PAAP (PA all-pathways); PAAI (PA IHI-Acute); PACI (PA IHI-Chronic); AIRP (air pathway); RFLX (radon flux).

The coefficient of variation (cvar) provides a measure of normalized spread within each histogram distribution. This spread has two potential sources: (1) uncertainty in a DU's closure composition; (2) uncertainty in waste generator inventories. The first source applies to open and future DUs

only, while the second source applies to all DUs. As Table 9-21 and Figure 9-35 indicate for the ELLWF, the spread for gross-alpha is greater than for beta-gamma.

9.1.2.4.3.3. Dose and Concentration Profiles

In contrast to Section 9.1.2.4.1, which focused on a single deterministic run, transient dose and concentration (history) profiles are computed for each DU, exposure pathway, and MC realization. This section presents a subset of the results for just one of the MC realizations, while Appendix I, Sections I.4.2.1 and I.4.2.2, provide the complete set of results for this one MC realization. The MC realization selected corresponds to the case where the maximum total SOF for the ELLWF occurs.

Detailed history profiles have been created for the MC realization yielding the peak overall SOF. For example, the dose history time profiles for ST24 (left) and ET08 (right) are displayed in Figure 9-37 [black-dashed curves based on Eq. (9-13)] for the beta-gamma GW pathway. The top-ten, rank-ordered parent radionuclide contributors are also shown [various colored curves based on RHS term in Eq. (9-13)]. A complete set of similar plots for every other DU and pathway is included in Appendix I, Section I.4.2.2.

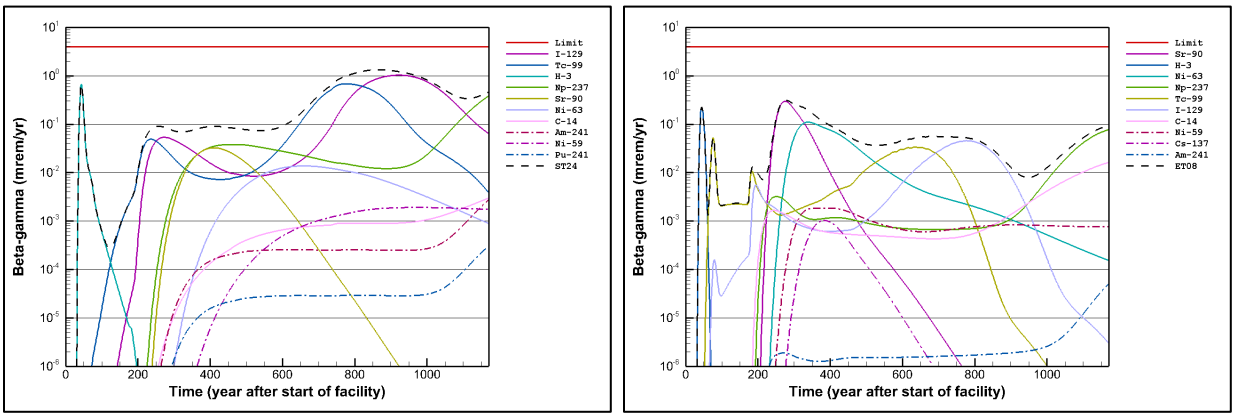

Figure 9-37. Stochastic Beta-Gamma Doses for ST24 and ET08 and Top-Ten Contributing Radionuclides

In the MC realization yielding the peak overall SOF, beta-gamma peak doses for ST24 and ET08 (Figure 9-37) are as follows:

- **ST24:** Maximum total dose = 1.335 mrem yr^{-1} in Year 864 (I-129 top contributor)
- **ET08:** Maximum total dose = 0.313 mrem yr^{-1} in Year 277 (Sr-90 top contributor)

As Figure 9-37 illustrates, a small subset of parent radionuclides generally dominates the maximum total dose for a given DU by exposure pathway.

Similarly, Figure 9-38 displays the concentration history time profiles for the gross-alpha GW pathway for ST24 and ET08 for the same peak MC realization.

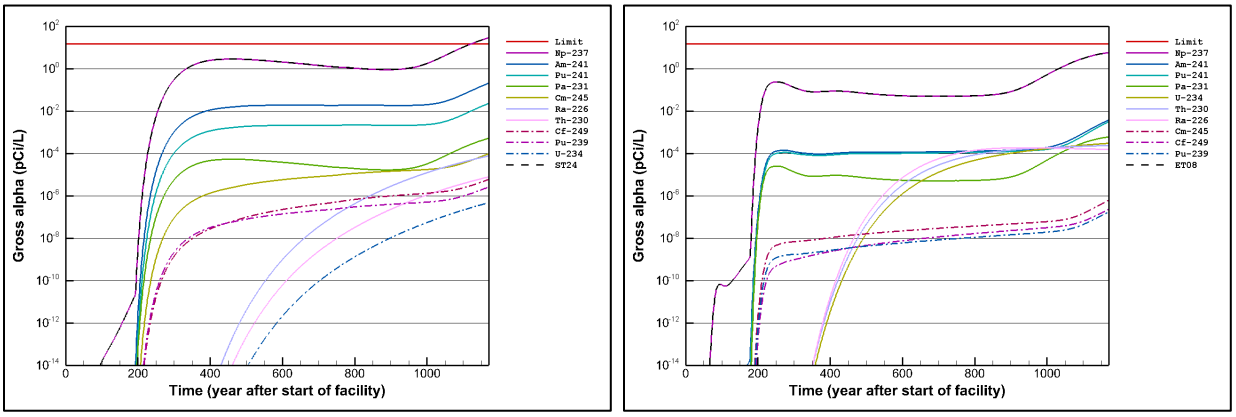

Figure 9-38. Stochastic Gross-Alpha Concentrations for ST24 and ET08 and Top-Ten Contributing Radionuclides

Gross-alpha peak concentrations for ST24 and ET08 per Figure 9-38 are as follows:

- **ST24:** Maximum total concentration = 29.4 pCi L^{-1} in Year 1,171 (Np-237 top contributor)
- **ET08:** Maximum total concentration = 5.8 pCi L^{-1} in Year 1,171 (Np-237 top contributor)

Note that for this specific MC realization, the projected closure inventories (projected CWTS inventories with biases plus uncertainties) for ST24 result in an exceedance of the 15 pCi L^{-1} PO (SOF = 1.96).

As an example of a non-GW pathway for the same peak MC realization, IHI-Chronic dose history time profiles for ST24 and ET08 are shown in Figure 9-39.

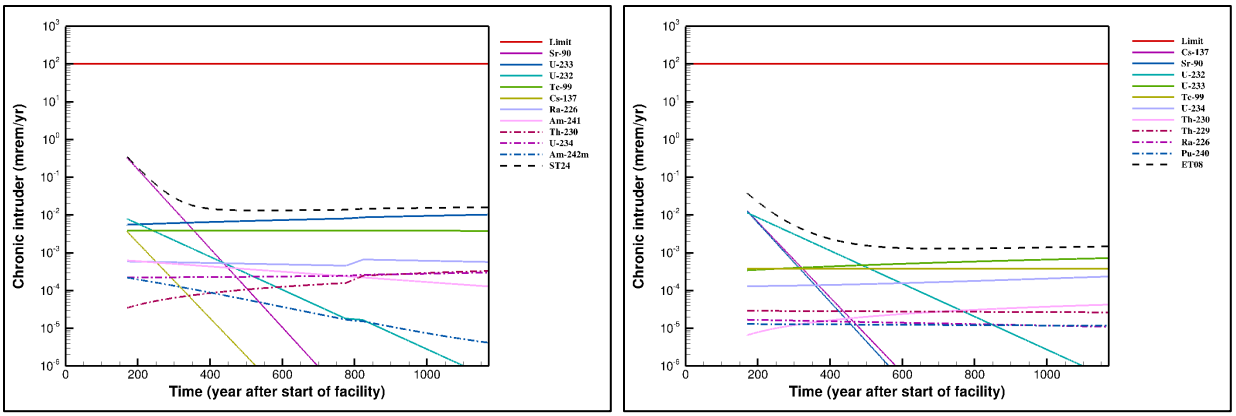

Figure 9-39. Stochastic IHI-Chronic Doses for ST24 and ET08 and Top-Ten Contributing Radionuclides

IHI-Chronic peak dose for ST24 and ET08 per Figure 9-39 are as follows:

- **ST24:** Maximum total dose = 0.352 mrem yr^{-1} in Year 171 (Sr-90 top contributor)
- **ET08:** Maximum total dose = 0.038 mrem yr^{-1} in Year 171 (Cs-137, Sr-90, and U-232 are top contributors)

Figure 9-40 shows the maximum total dose for the beta-gamma GW pathway for the overall ELLWF (solid-black curve). The top-ten DU contributors are displayed in the left image while only ST24 and ST01 are shown in the right image. ET08 is not shown because it is not a top-ten contributor .

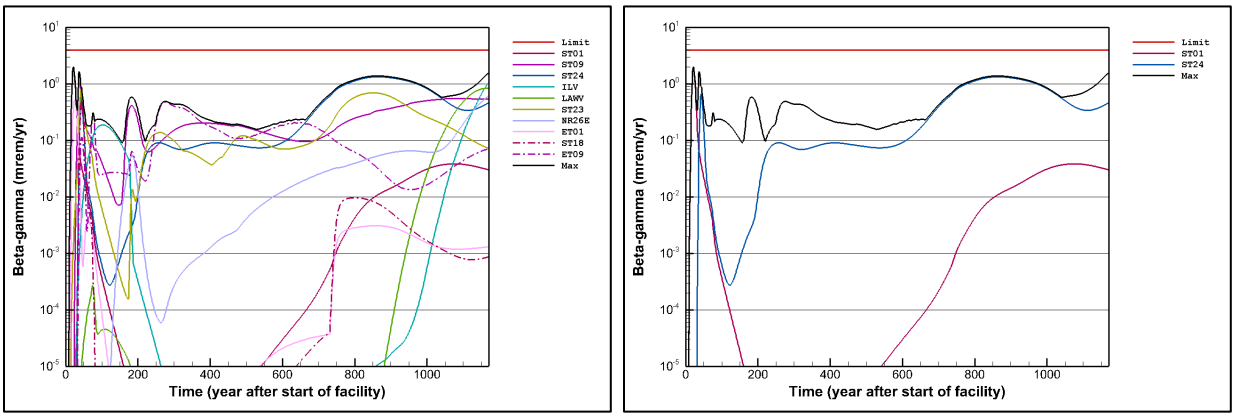

Figure 9-40. Stochastic Total Beta-Gamma Doses for ELLWF and Top-Ten Contributing Disposal Units

The key beta-gamma peak doses for the overall ELLWF (Figure 9-40) are as follows:

- **ELLWF:** Maximum total dose = 1.989 mrem yr^{-1} in Year 21 (ST01 top contributor)
- **ST01:** Maximum total dose = 1.988 mrem yr^{-1} in Year 21 (H-3F top contributor)

The dose highlighted in orange above for the ELLWF represents the peak beta-gamma dose at the North curtain for the selected MC realization. A complete set of similar plots for every exposure pathway is provided in Appendix I, Section I.4.2.1.

9.2. USE OF PERFORMANCE ASSESSMENT RESULTS

This PA is being used to comply with DOE O 435.1, Chg 2: 1-11-2021 (U.S. DOE, 2021a), which requires radioactive waste to be managed in accordance with DOE M 435.1-1, Chg 3: 1-11-2021 (U.S. DOE, 2021b). Specifically, this PA is developed to meet the requirement that an assessment be prepared and maintained for DOE LLW disposed after September 26, 1988. Additionally, this PA is developed in accordance with DOE-STD-5002-2017 (U.S. DOE, 2017). The results of this PA provide a reasonable expectation that the facility design and method of disposal will comply with the POs in DOE M 435.1-1, Chg 3: 1-11-2021 (U.S. DOE, 2021b), which ensure protection of public health and the environment by limiting doses to a MOP and limiting releases of radon. The PA also provides reasonable expectation that the applicable POs of 10 CFR Part 61 (NDAA, 2004) will be met. In addition, this PA assesses impacts to a hypothetical IHI and water resources.

Primary applications of the PA2022 results are as follows:

- Establish parent radionuclide disposal (inventory) limits for each DU employed in daily operations. The inventory limits are directly used in establishing estimated facility closure inventories for all DUs within the ELLWF. The inventory limits can be found in Chapters 7

and 8 as well as Appendices G and H. Upon approval of this PA, a separate Microsoft Excel spreadsheet will be generated containing all inventory limits on a time window basis for every DU and exposure pathway of interest. The preparation of this spreadsheet will be part of the Performance Assessment Implementation Plan.

- Produce a facility closure analysis that provides assurances that operations prior to closure are maintained within a posture that results in a low probability of exceeding POs during ongoing operations and beyond for a reasonable period of performance. To assess these objectives, both deterministic and stochastic analyses are performed.
- Provide guidance on ongoing maintenance activities and operational constraints as dictated by the key PA modeling assumptions utilized in generating the inventory limits (see Appendix A, Table A-4). Therefore, PA2022 will be used to assist in decision-making related to operations and waste disposal within the ELLWF.

The inventory limits calculated in PA2022 are implemented through a set of WAC and managed through SRS's computerized CWTS (SRS, 2021c). The SRS Radioactive Waste Requirements 1S Manual (SRS, 2021d) provides actions to be taken, for example, to:

- Ensure that DOE LLW at SRS is managed in accordance with the requirements of DOE O 435.1, Chg 2: 1-11-2021 (U.S. DOE, 2021a) and DOE M 435.1-1, Chg 3: 1-11-2021 (U.S. DOE, 2021b) in accordance with the applicable requirements of external regulations.
- Provide requirements associated with the development of suitable methodologies for characterization of waste packages and establishes the basis to ensure that all LLW packages presented to SWM for disposal have been characterized by the waste generator to reasonably represent the physical, chemical, and radiological contents of the waste package with sufficient accuracy to permit proper disposal.

CWTS is used to input, store, analyze, and generate reports in an automated manner with the intent of reducing the potential for human errors and disposals failures. SWM has demonstrated over the years that the CWTS program has the appropriate capabilities to properly protect the critical inventory limits and manage the available disposal resources in the most cost-effective manner. Experience has generally proven that the LLW radiological inventories typically generated at SRS are properly characterized and managed into the appropriate disposal locations.

The operating limits for the ELLWF, as documented in the SRS Radioactive Waste Requirements 1S Manual (SRS, 2021d), are derived from safety documentation and the PA. SRS (2021d) compiles radionuclide limits from a DSA, criticality limits, 100 nCi g^{-1} transuranic concentration limit, and performance-based inventory limits. Key WAC examples for the ELLWF are as follows (see Appendix A, Table A-4, for a more complete listing):

- **5% PA Package Screening Limit:** Established to protect a key PA modeling assumption that the radionuclide inventory in each SWM disposal facility is uniformly distributed. Failure of this limit indicates that a potential "point source" disposal inventory may exist, which is prohibited without additional analysis. A 0.5% PA (administrative) package screening limit

has been established by SWM as an administrative management tool so as to identify waste containers with a significant inventory contribution for a given disposal location.

- **Non-Crushable Container Screening Limit:** Established to protect a key PA modeling assumption that the upper-bound degree of subsidence (beyond the end of IC) within a particular DU is not exceeded. Failure of this limit indicates the potential for higher infiltration rates over a larger portion of the waste zone, which is prohibited without additional analysis.

As packages are received for emplacement in the various types of DUs (ST, ET, LAWV, ILV, and NRCDA), their package contents are entered into CWTS. Before emplacement of each package, CWTS will compare the package contents with the 100 nCi g^{-1} transuranic limits and calculate the inventory (to ensure compliance with the criticality limits) and the total disposal inventory (to ensure compliance with the PA-based limits). The DSA- and PA-based limits are tracked as a SOF of the individual radionuclide limits. A separate SOF is calculated for the air pathway, radon pathway, each relevant IHI scenario, and separate time windows for the GW pathways, as appropriate. For the PA-based limits, the total DU inventory for each radionuclide is divided by its corresponding limit for each of these calculations. The sum of these fractions is maintained less than 1.0 (or some lower administrative limit such as 0.95) to ensure compliance with the limits and, thus, the POs. Temporary lower administrative limits have been historically employed while follow-on UDQEs and SAs are considered.

The inventory limits reported in Chapter 8 employ GW time windows, while compliance is maintained using a SOF rule. An example of the CWTS application of these concepts is provided in Appendix H, Section H.8. Briefly, inventory limits are developed by ratio of the maximum impact (e.g., all-pathways dose) calculated for a specific time period for a unit inventory of each radionuclide to the respective PO (e.g., 25 mrem yr^{-1}). The PA-derived limits are expressed in terms of curies per DU. For the GW pathway, which is generally the most limiting, the time period for the analysis is subdivided into multiple periods; limits are then derived for each period. These non-overlapping time periods are established to separate impacts from GW peaks that occur at different times, which reduces the conservatism in the SOF of limits method for assessing compliance.

The PA sensitivity analysis and uncertainty quantification results (see Chapter 6) also help determine (and prioritize) where future PA maintenance activities should focus (i.e., what disposal facility parameters). These activities may include development of more rigorous analytical techniques for radionuclide activity levels or enhanced efforts to more accurately quantify environmental, or other physical, parameters.

9.3. FUTURE WORK

DOE M 435.1-1, Chg 3, IV.P.4 (U.S. DOE, 2021b) includes a requirement for PA maintenance to evaluate changes that could affect the performance, design, and operating basis for the facility. This maintenance program shall include the conduct of research, field studies, and monitoring needed to address uncertainties or gaps in existing data. Under this program, PA2022 will be reviewed annually for changes in waste forms or containers, radionuclide inventories, facility

design and operations, closure concepts, or the improved understanding of the performance of the ELLWF in combination with the features of that area of SRS on which it is located. Based on these annual reviews, a determination will be made as to the continued adequacy of this new PA with respect to sustained operation of the facility under the current DAS. Annual summaries of ELLWF operations will be prepared with respect to the conclusions and recommendations of the current PA and a determination of the need to revise that document.

The most recent ELLWF PA Maintenance Plan (Crawford, 2021) includes a description of the following ongoing R&D field investigations arising from PA2008:

- Survey CIG grout test pour for potential cracking to validate PA assumptions.
- Monitor SRNL radionuclide field lysimeter experiment for specific K_d values.
- Assess data from B-25 box corrosion monitoring field site to validate PA assumptions.

The above three investigations will likely continue in the future.

Based on the technical efforts employed during the development and completion of PA2022, six DUs (i.e., ET06, ST17, ST19, ST20, ST21, and ST22) were identified as potentially being excluded from future use because of significantly reduced disposal capacities that are primarily attributed to the simulated, recalibrated aquifer flow fields beneath ELLWF and the associated PIPs. Future analyses may be able to reclaim this reduced disposal capacity. A stochastic analytical approach, instead of the current PIF approach, may be able to recover the lost disposal capacity.

9.4. REFERENCES

Crawford, K. C. (2021). "Maintenance Plan for the E-Area Low-Level Waste Facility (ELLWF) Performance Assessment (PA)." SRNS-N3000-2021-00016. Savannah River Nuclear Solutions, Savannah River Site, Aiken, SC. April 20, 2021.

Hamm, L. L., Aleman, S. E., Danielson, T. L., and Butcher, B. T. (2018). "Special Analysis: Impact of Updated GSA Flow Model on E-Area Low-Level Waste Facility Groundwater Performance." SRNL-STI-2018-00624, Rev. 0. Savannah River National Laboratory, Aiken, SC.

Hamm, L. L., Smith, F. G., Flach, G. P., Hiergesell, R. A., and Butcher, B. T. (2013). "Unreviewed Disposal Question Evaluation: Waste Disposal In Engineered Trench #3." SRNL-STI-2013-00393, Rev. 0. Savannah River National Laboratory, Aiken, SC.

NDAA (2004). Subpart C of 10 CFR Part 61, Licensing Requirements for Land Disposal of Radioactive Waste. *In* "Ronald W. Reagan National Defense Authorization Act for Fiscal Year 2005, Section 3116," Washington, DC. October 2004.

SRS (2021c). "Requirements Specification for Software for the Consolidated Waste Tracking System (CWTS)." B-RS-G-00107, Rev. 2. Savannah River Nuclear Solutions, Savannah River Site, Aiken, SC.

SRS (2021d). "SRS Radioactive Waste Requirements Manual: Low-Level Waste." SRS Manual 1S, Chapter 5, Rev. 2. Savannah River Site, Aiken, SC. February 11, 2021.

Taylor, S., and Whiteside, T. S. (2022). "E-Area Low Level Waste Generator Inventory Uncertainty Estimation." SRNL-STI-2021-00276, Rev. 0. Savannah River National Laboratory, Aiken, SC. January 2022.

U.S. DOE (1999). "Implementation Guide for Use with DOE M 435.1-1, Chapter IV." DOE G 435.1-1. U. S. Department of Energy, Washington, DC. July 9, 1999.

U.S. DOE (2017). "Disposal Authorization Statement and Tank Closure Documentation." DOE-STD-5002-2017. U.S. Department of Energy, Washington, DC.

U.S. DOE (2021a). "Radioactive Waste Management." DOE O 435.1, Chg 2: 1-11-2021. U. S. Department of Energy, Washington, DC. Approved: July 9, 1999.

U.S. DOE (2021b). "Radioactive Waste Management Manual." DOE M 435.1-1, Chg 3: 1-11-2021. U. S. Department of Energy, Washington, DC. January 11, 2021.

Verst, C. (2021a). "Calculated Gamma Factors at Human Receptor Locations Near HWCTR and NR Cask Special Waste Forms in E-Area." SRNL-STI-2021-00307. Savannah River National Laboratory, Aiken, SC. June 2021.